Geological Field Trips and Maps

2023
Vol. 15 (1.4)

SOCIETÀ GEOLOGICA ITALIANA
FONDATA NEL 1881 - ENTE MORALE R. D. 17 OTTOBRE 1885

ISPRA
Istituto Superiore per la Protezione e la Ricerca Ambientale

Sistema Nazionale per la Protezione dell'Ambiente

ISSN: 2038-4947

Quaternary deformations, palaeosols and strata across the Northern Apennines

PRE-17 Pre-congress Field Trip of the XXI Inqua Congress "A Mediterranean perspective on Quaternary Sciences", Rome 14th-20th July 2023

https://doi.org/10.3301/GFT.2023.04

GFT&M - *Geological Field Trips and Maps*

Periodico semestrale del Servizio Geologico d'Italia - ISPRA e della Società Geologica Italiana
Geol. F. Trips Maps, Vol.**15** No.1.4 (2023), 47 pp., 23 figs., 5 tabs. (https://doi.org/10.3301/GFT.2023.04)

Quaternary deformations, palaeosols and strata across the Northern Apennines

PRE-17 Pre-congress Field Trip of the XXI Inqua Congress "A Mediterranean perspective on Quaternary Sciences", Rome 14th-20th July 2023

Anna Andreetta[1], Marco Benvenuti[1], Daniele Maestrelli[1], Stefano Carnicelli[1], Federico Sani[1]

[1] Dipartimento di Scienze della Terra, Università di Firenze

Corresponding author e-mail: anna.andreetta@unifi.it

Cover page Figure: Panoramic view of the Late Pliocene-Quaternary marine to continental deposits outcropping along the Enza River stratigraphic section (Stop 1.1, San Polo d'Enza), showing progressive unconformities as a result of the Pede-Appenine thrust activity (Photo courtesy of D. Maestrelli).

ISSN: 2038-4947 [online]

http://gftm.socgeol.it/

INDEX

INFORMATION

EXCURSION NOTES

ITINERARY

https://doi.org/10.3301/GFT.2023.04

ABSTRACT

The Northern Apennines chain is an active orogen developed in a continental collisional setting. During the Quaternary active tectonics, climate fluctuations, and sea-level change left a clear imprint on the regional geomorphology and the surface geology. Examination of stratigraphically correlated palaeosols within alluvial and coastal clastic successions occurring on both sides of the chain, i.e., on the active front (Northern slope) and the back-arc area (Tuscany), provide fine detail to reconstructions of the orogen dynamic during the Quaternary. Examples of dated and correlated palaeosols within their morpho-structural, stratigraphic, and sedimentological context, will be presented and discussed on the Northern side of the chain (Ghiardo plateau, in the picture) and in the coastal Tuscany (Baratti gulf). In the transfer from the northern slopes to the back-arc area, selected stops in the Pleistocene fluvio-lacustrine Mugello basin will provide a sight into the morpho-stratigraphic architecture of an intermontane basin developed in the axial portion of the Northern Apennines.

Key words: Northern Apennines, Palaeosols, active tectonics, thrust top basins, Palaeoenvironment, Pede-Apennine Thrust, Ghiardo Plateau, Mugello Basin, Baratti.

PROGRAM SUMMARY

The field trip is organised as a transect through the Apennine chain, starting from the external sectors, crossing the main divide, and reaching the Tuscan coast.

DAY 1 and **DAY 2**: During the first and second days we will provide a general overview of an active sector of the pede-Apennine margin and its adjoining areas. We will visit outstanding outcrops occurring along the Enza River valley (close to the S. Polo d'Enza City; Day 1 in Fig. 1), showing a growth fold associated with the activity of the pede-Appennine Thrust (PAT) and involving marine and fluvio-deltaic Quaternary deposits intercalated with palaeosols.

The second day will be devoted to the observation in the Quattro Castella area, and the deformation associated with an anticline, this latter connected at depth to a thrust ramp. The forelimb of the anticline is affected by well-developed faceted spurs that reach at place a height of 50 m. Climbing the foothill, a panoramic spot will open us the view of the plain standing in front of the morphological margin: this panorama will allow us to observe a topography interpreted to be the result of recent uplift, likely connected with the deformation of a buried thrust fault splaying from the main pede-Apennine thrust previously observed. This structural and morphological high allowed the formation of a small plateau (Ghiardo Plateau). As the plateau is covered by complex palaeosols, the opening of a soil profile will provide a great opportunity to show their evidence and to discuss about their implication for the interpretation of the structural evolution of the pede-Apennine margin.

DAY 3: During the third day we will cross the chain and we will observe the Mugello intermontane basin, which represents one of the most external basins of the inner side of the Northern Apennines (Fig. 1). This basin has a complex stratigraphic evolution controlled at the beginning of its formation (Early Pleistocene) by compressive tectonics and later developing prominent, still active, normal faults. The stratigraphic succession and the associated palaeosols will be the object of the stops.

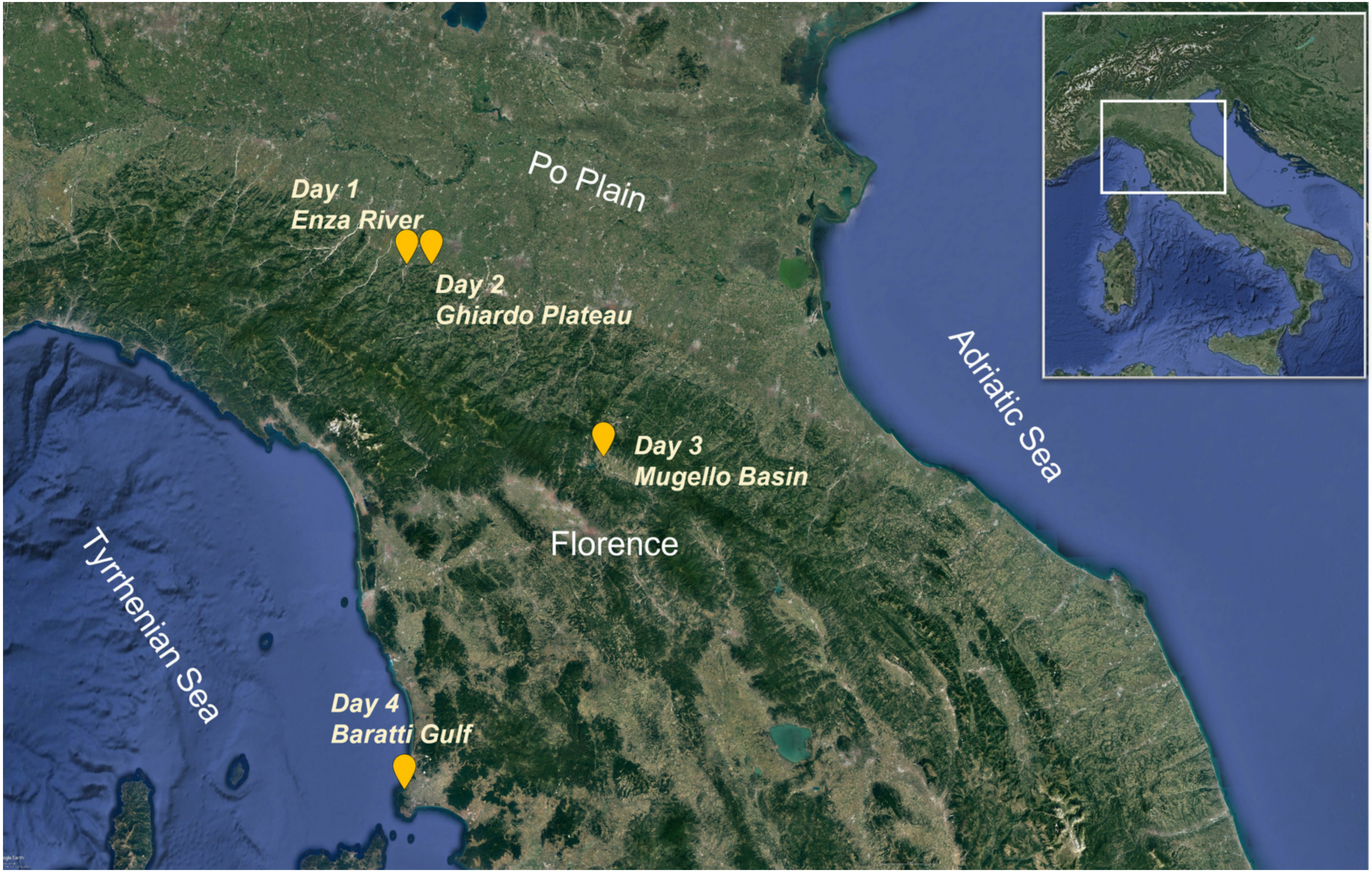

Fig. 1 - Google Earth view of the field trip itinerary.

https://doi.org/10.3301/GFT.2023.04

DAY 4: The fourth day of the field trip will focus on the coastal area of Baratti, 80 km south of Leghorn (Fig. 1), bearing in the cliffs bounding the embayment the stratigraphic record of an articulated evolution controlled by climate and sea-level variations. Outcrops visited in this stop will integrate stratigraphic and sedimentological observations with pedofeatures to re-examine a classic Quaternary section.

SAFETY

Safety in the field is closely related to self-awareness. Most of the outcrops are along roads and paths that generally are well-maintained. Some outcrops are reached by driving along sinuous roads. We highly recommend wearing walking mountain boots, bringing sun protection, hats or headscarves, and sunglasses. Northern Italy in summer can be really hot. We recommend bringing drinkable water. Locally, rain showers can occur in any season. Mobile/cellular phone coverage is generally good.
Useful phone numbers
112: European Emergency Number
118: Pronto Soccorso (First aid)
115: Vigili del Fuoco (Firefighters)
113: Polizia (Police)

HOSPITALS

Arcispedale S. Maria Nuova, Viale Risorgimento, 80 Reggio Emilia, 0522 296111.
Nuovo Ospedale del Mugello, viale della Resistenza 60 - Borgo San Lorenzo (Firenze) 055 84511.
Ospedale della Misericordia, Via Senese 161 Grosseto 0564 485111.
Emergency call everywhere in Italy is 112.

OVERNIGHT ACCOMMODATION

The proposed stops are next to touristic facilities that include overnight accommodation.

GEOLOGICAL SETTING OF THE NORTHERN APENNINES

The Northern Apennines (NA) constitute an arc-shaped chain composed of a pile of NE- to E-verging tectonic units and associated second-order back-thrusts (Fig. 2).

The NA are made up of two main groups of tectonic units deriving from two distinct palaeogeographic domains: (1) the Ligurian units, representing allochthonous terrains scraped from the original oceanic crust (ophiolites and overlying Jurassic to Eocene sedimentary cover of the Ligurian–Piedmont, or Alpine Tethys Ocean) and (2) the Tuscan and Umbria–Marche units, constituting the sedimentary cover of the western thinned continental margin of the Adria Plate.

The Ligurian units are composed of ophiolites coupled with their Jurassic to Eocene sedimentary cover, and tectonically overlie the Tuscan and Umbria–Marche units, originally deposited on the passive margin of the Adria Plate since the Middle Triassic. The Tuscan and Umbria–Marche units consist of a lower succession of Mesozoic–Cenozoic age, mainly composed of carbonate rocks and of an upper, 2000–3000-m-thick, succession of Oligocene – Miocene age, formed by siliciclastic foredeep sediments. Both successions rest on about 1000–1500-m-thick Triassic evaporites (Anidriti di Burano Fm.). Within the evaporitic layer is located one of the most important detachment levels of the NA. The Mesozoic sequence shows a slight variation moving outward, suggesting a gradual facies transition. Due to time–space outward migration of the thrust front, Oligocene–Miocene siliciclastic turbiditic formations accumulated in the foredeep become progressively younger eastwards. From west to east, these units are the Macigno, Cervarola–Falterona, and Marnoso–Arenacea units.

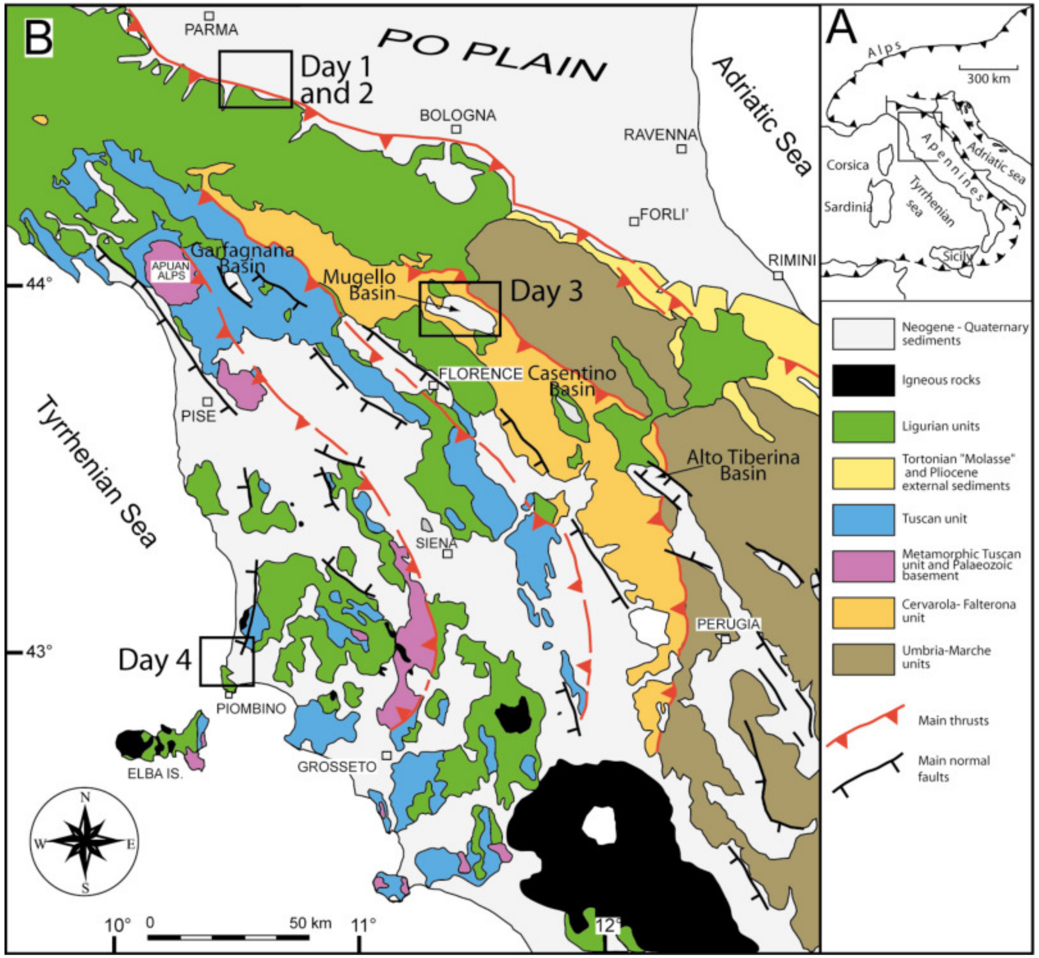

Fig. 2 - Geological map of the Northern Apennines. Insets represent the areas visited during the fieldtrip.

The deformation of the NA started in the Late Cretaceous as a consequence of the Alpine Tethys Ocean closure. Two different interpretations of the subduction polarity of the Alpine Tethys have been proposed: (1) a west-dipping subduction below the Corsica–Sardinia block (which

https://doi.org/10.3301/GFT.2023.04

was still connected to the European margin) (Scholle, 1970; Abbate et al., 1986; Bortolotti et al., 2001, 2005, and reference therein); and (2) an east-dipping oceanic lithospheric subduction below the Adria Plate postulated by Boccaletti and Guazzone (1970; 1972; 1974) and Boccaletti et al. (1971). According to this latter hypothesis, the Apennine orogeny *s.s.* started after the continental collision, i.e., at the end of the late Oligocene (Boccaletti et al., 1980, see also Marroni et al., 2017 and reference therein). Following the Ligurian–Piedmont Ocean closure, the rotation of the Corsica–Sardinia block started together with the opening of the Balearic basin to the west (Dewey et al., 1973; Biju Duval et al., 1977; Burrus, 1984; Finetti and Del Ben, 1986). The time–space migration toward the east and northeast of the foredeep system has been commonly associated with this rotation.

Currently, the NA chain, from east (foreland) to west (hinterland), can be schematically subdivided into three sectors (Fig. 2): (i) a buried belt below the Po Plain, where the thrust system, mainly Pliocene–Quaternary in age, is still active; (ii) a central belt, coinciding with the Apennine chain *s.s.*, where the thrust system, mainly formed in the Late Miocene–Pliocene, shows still an active compression at depth (>15km), but is affected by active extensional deformation at more superficial levels (< 15 km), and (iii) an internal belt where continental or marine basins formed since the middle–late Tortonian as thrust top basins and was later affected by extensional tectonics (Boccaletti et al., 1999; Bonini et al., 1999, 2014; Sani et al., 2016).

Following the field trip itinerary, these three sectors will be briefly described below.

The external sector of the Northern Apennines is characterised by active shortening, accommodated by folding and thrusting (e.g., Benedetti et al., 2003; Boccaletti et al., 2004; Martelli et al. 2017a, b; Amadori et al., 2019; Zuffetti and Bersezio, 2020; DISS Working Group, 2021). Current activity results are well constrained by earthquake fault plane solutions, seismic sections, and geodetic analysis (Figs. 3, 4; e.g., Pondrelli et al., 2006; Chiarabba et al., 2005; Serpelloni et al., 2005; 2007; D'Anastasio et al., 2006; Piccinini et al., 2006; Montone et al., 2012; Livani et al., 2018; Maestrelli et al., 2018; Amadori et al., 2019).

The Po Plain is characterised by buried active thrusts and folds affecting the 7- to 8-km-thick Plio-Quaternary infill, giving rise to the typical arcuate systems of buried folds (the so-called Emilia and Ferrara folds; Fig. 3; Pieri and Groppi, 1981) whose activity is possibly connected to surface faulting events (Pellegrini and Vezzani, 1978; Martelli et al., 2017a, b; Zuffetti and Bersezio, 2020). Late Quaternary deformation is clearly highlighted by the interpretation of high-resolution seismic data and seismic activity (Fig. 4; e.g., Boccaletti et al., 2004b; Scrocca et al., 2007; Martelli et al., 2017a, b; Maestrelli et al., 2018; Amadori et al., 2019).

The transition between the Po Plain and the Apennine chain *s.s.* coincides with the pede-Apennine margin representing the hinge between the chain and the buried sectors of the collisional belt (Maestrelli et al. 2018; Figs. 2, 3).

In the Apennine chain, the active deformation is taken up by a major system of thrust faults, developing in correspondence and parallel to the main Apennine divide (Figs. 2, 3). Deformation on these structures gives rise to main "tectonic windows", out-of-sequence structures, and local growing anticlines characterised by strong morphotectonic signatures revealing their recent activity, with the presence of prominent faceted spurs, wind gaps, hanging valleys, river captures (Boccaletti et al., 2004; Martelli et al., 2017a, b; Molli et al., 2018).

https://doi.org/10.3301/GFT.2023.04

Fig. 3 - (a) Main structural features of the study area modified from Maestrelli et al. (2018). The emergent and buried main thrust fronts are reported. (b) Schematic stratigraphic columns of the marine and continental Pleistocene deposits outcropping in the study area. FAA: Argille Azzurre formation; ATS: Torrente Stirone Synthem; IMO: Imola Sands; AEI: Lower Emilia-Romagna Synthem; AES: Upper Emilia-Romagna Synthem; ADO: Monte Adone Formation. Ages are from Cerrina Feroni et al. (2002) and Gunderson et al. (2014). Black box indicates the area shown in Figure 5.

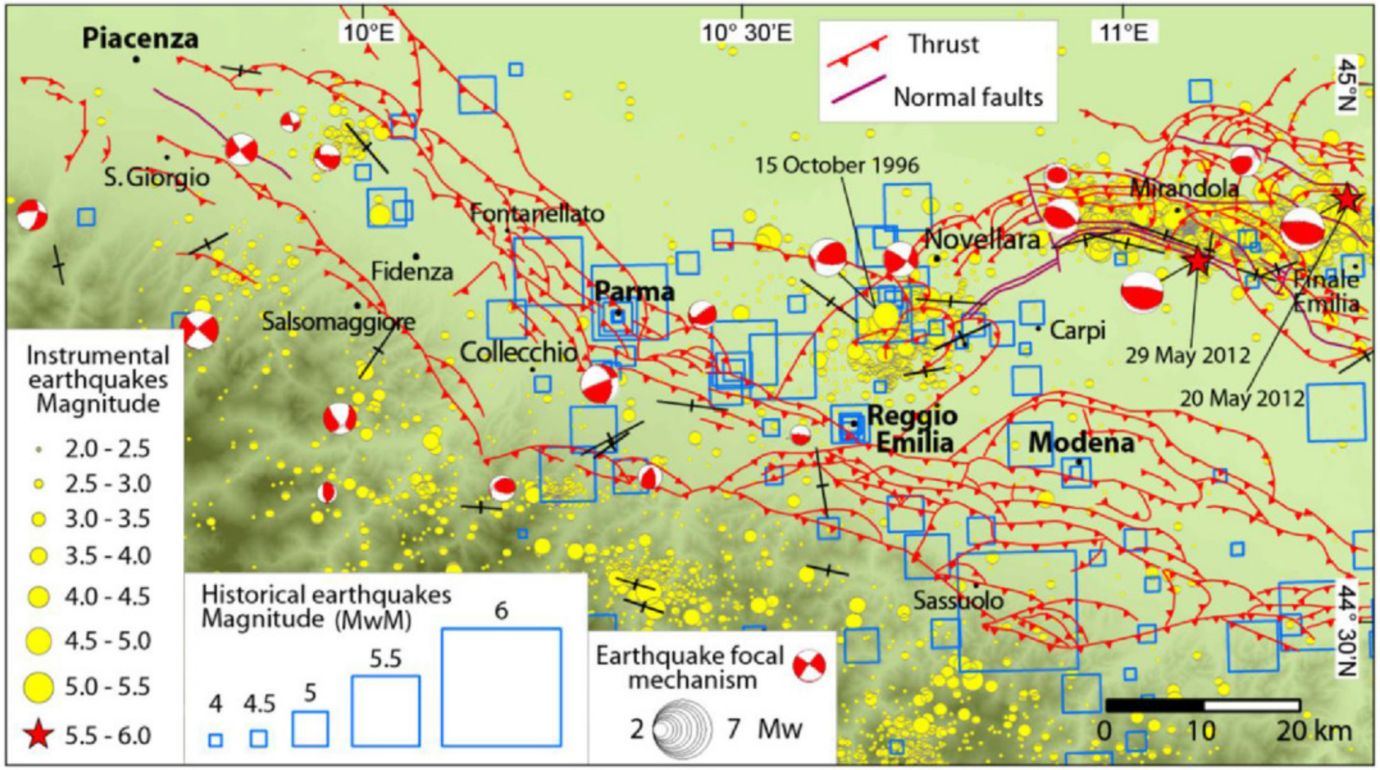

Fig. 4 - Seismotectonic map of the area. The main structural elements are modified from the Structural Model of Italy (Bigi et al., 1983). From Antonielli (2015).

The NA chain in the divide area constitutes the major outcropping fold and thrust belt and it is composed of thrust faults and associated folds displaying a complex structure related to the advancing chain that progressively involved foredeep sediments. This process determined a strict relation between tectonics and sedimentation and the involved formations often show growth folding and other characteristics attesting a tectonically active context of sedimentation. After the major phases of mountain chain building, in the divide area developed Early Pleistocene intermontane basins that, from the NW, are the Garfagnana, Mugello, Casentino, and Alto Tiberina Basins (Fig. 2). The Mugello Basin is inferred to have developed in Early Pleistocene under a compressive regime and was later affected by normal faults as the compressive regime ceased around the Early-Middle Pleistocene transition (Sani et al., 2009a). Currently, the Mugello is one of the more seismically active areas of this external belt and its seismicity shows a high variability in terms of intensity, depth, and kinematics (Bonini et al., 2016). The seismicity shows extensional kinematics and it is related to a ~25–30 km long SSW-dipping normal fault system referred to as the "Ronta fault system" that delimits the northeastern basin margin. These structures show mainly dip-slip kinematics and display remarkable morpho-structural evidence (Sani et al., 2009a; Bonini et al., 2016; Saccorotti et al., 2022).

The southwestern margin of the basin is also affected by NE-dipping antithetic normal faults, with less pronounced morphologic expression (Benvenuti and Papini, 1997; Sani et al., 2009a). The asymmetric location of the Sieve River on this side of the basin is believed due to the activity of these structures (Benvenuti and Papini, 1997). Previous studies locate the basin master fault along this margin (Martini and Sagri, 1993), and other authors connect these structures to a regional NE dipping low-angle normal fault (Boncio et al., 2000).

https://doi.org/10.3301/GFT.2023.04

The hinterland sector of the NA is normally referred to as a back-arc area including the Tyrrhenian Basin and many marine and continental basins developed since the Middle-Late Miocene in the current onshore of Tuscany (e.g., Boccaletti and Guazzone, 1972; Malinverno and Ryan, 1986; Doglioni, 1991; Faccenna et al., 2001; Carminati and Doglioni, 2012).

The evolution of these marine and continental hinterland basins has been classically referred to an extensional regime, associated with the back-arc-related Tyrrhenian Basin opening, which gave rise to grabens and half-grabens bounded by high-angle normal faults since the late Tortonian (e.g., Martini and Sagri, 1993, and references therein).

This interpretation has been questioned since field investigations have indicated a more complex tectono-sedimentary evolution for the Tortonian–Early Pleistocene hinterland basins and a model in which the basins developed mainly under compressive conditions has been proposed (Boccaletti et al., 1999; Bonini and Sani, 2002).

Indeed, despite of a thin continental crust (~20–25 km in the hinterland vs. 35–45 km toward the foreland; Cassinis et al., 2005), the presence of magmatism (Serri et al., 1993), and related high heat flow (>100 mW m^{-2}, which in geothermal areas may exceed 250 mW m^{-2}; Mongelli et al., 1998; Della Vedova et al., 2001), various geophysical data show that the hinterland continental crust is considerably shortened by thrust faults (Arisi Rota and Fichera, 1985; Bally et al., 1986; Ponziani et al., 1995; Cassano et al., 1998; Scarascia et al., 1998; Finetti et al., 2001).

Moreover, systematic structural studies carried out on several hinterland basins integrated with detailed sedimentological–stratigraphic studies, have allowed the recognition that the basins infill dominantly developed in a compressional setting (e.g., Moratti and Bonini,1998; Boccaletti et al., 1999; Bonini et al., 1999; Bonini and Sani, 2002; Sani et al., 2009a, b; Benvenuti et al., 2014). These studies allowed the identification of some common features found in the hinterland basins of the Northern Apennines: (i) location between thrust anticlines in the substratum and a general synformal shape; (ii) presence of progressive unconformities at the basin margins, attesting syn-depositional uplifting of the margins (e.g., Riba, 1976; Zapata and Allmendinger, 1996); (iii) significant compressive deformation affecting the basin fill, whose stress fields are coherent with the trend of the major structures of the substratum at the basin margins; (iv) when present, high-angle minor normal faults represent recent features unrelated to basin formation and not controlling sedimentation within the basin (Sani et al., 2009b; 2016; Bonini et al., 2013, 2014); on the contrary, normal faults are in most cases, situated on the rear of the thrust anticlines, accommodating thrusting process.

During the Quaternary active tectonics, climate fluctuations and sea-level change, interacting and competing with each other, left a clear imprinting on the regional geomorphology, the surface geology, and correlated palaeosols within alluvial and coastal clastic successions occurring on both sides of the chain.

THE USE OF PALAEOSOLS IN STRATIGRAPHY

The significance of buried palaeosols as stratigraphic unconformities is long acknowledged (NACSN, 2005). It is, however, useful to further analyse the kind of record represented by palaeosols. As a fundamental difference from other types of unconformities, palaeosols define a "conservative" unconformity; their presence indicates that no erosional event has taken place at the time they mark as a stratigraphic boundary. More correctly, it should be said that a limited amount of erosion may have happened, as buried palaeosols may easily be found in a truncated form, only the deeper horizons having been preserved. This observation takes more significance when stratigraphic analysis is carried out to reconstruct structural phases. Here, the difference between "conservative" and erosional unconformities shows whether a given stratigraphic boundary has been accompanied by the significant shifts of base level that occur as a consequence of significant deformation, or not.

Another kind of information that can be found in palaeosols, either buried or relict, is the possibility of tracing depositional events that have produced thin beds, which subsequently have been subjected to weathering and have come to be part of what is initially perceived as a single soil profile, but that, on a more careful observation, turns out as being a composite geosol (NACSN, 2005). The importance of a stratigraphic bed is not necessarily dependent on its thickness; significant information can then be obtained by the ability to disentangle composite palaeosols.

Finally, we should not limit our look to buried palaeosols. Naturally, relict (surface) palaeosols present much greater interpretation problems, as they contain multiple sources of ambiguity. However, their potential value is given by the fact that they may allow correlating significant stratigraphic boundaries with present-day topographic surfaces (Benvenuti et al., 2002; Sagri et al., 2008), thus shedding much light on the nature and timing of landforms, a data which is, again, very useful in reconstructing structural evolution.

RECOGNISING PALAEOSOLS

While identifying relict palaeosols may be complex and ambiguous, their existence is quite often noted in soil maps and databases, as their identification and characterisation remain a task of Pedology. Palaeosols stacked within sedimentary clastic, or volcanic successions present a different problem; in the first place, they will only be "found" by geologists, not by pedologists. Moreover, while a relict soil is obviously a soil, the first problem within a succession is acknowledging the presence of a soil. Thus, the issue of which characters allow to recognise, or at least to suspect, the presence of a deeply buried soil is important.

Typically, some "beds" within a succession may show suspect characters. Which such characters mark a deeply buried palaeosol? The basic concept is that soils are sets of surface-driven modifications to which any rock body may be subjected. The first "suspect" character is the disappearance of such macroscopic rock features as texture, structure, and facies. There are indeed important cases in which the only divide between noncoherent rock and soil is the emergence of soil structure, which is amply described in such standard sources as Schoeneberger et al. (2012) and USDA-NRCS (2012). As for all the characters we are describing, however, soil structure is not always preserved in deep burial. Another significant character is colour; blackish or reddish-yellow colours are often typical of soils, though there are exceptions. Highly significant may indeed be the presence of mottled colours, with spots of contrasting greyish and reddish colours, induced by redox phenomena within soils. Almost always coming from soil processes are mottling patterns oriented vertically or of reticular shape, while much caution needs to be used when mottling is dominantly horizontal. Chemical weathering is a major soil-forming process, though soils exist also with no or minimum chemical weathering. Assessing chemical weathering in the field may be very tricky, but this is no problem when coarse clasts are present. Weathered portions are easily lost in transport, so the presence of weathered coarse clasts within a succession may be a very robust indicator of significant weathering *in situ*.

NOTES FOR THE SOIL DESCRIPTIONS WITHIN THIS GUIDE

We then emphasise practical observations that can be useful to better understand the description and discussion of palaeosols encountered in this field excursion. The basic soil observation entities are horizons, a term used to avoid ambiguity with the concepts of beds and strata. Although soil horizons and geological beds can look similar, their origin is fundamentally different. As soil formation occurs, the resulting properties appear in different ways according to the distance from the surface. However, each horizon is not only seen as an individual but as a member of a “sequence” (*solum*). To tag soil horizons, a formal method has been developed, which follows an alphanumeric code. Briefly, master horizons are designated with capital letters: O, A, E, B, and C. Lowercase letters are used as descriptors in conjunction with master designations to connote specific characteristics. The principal suffixes used for the palaeosols presented in this guide are reported in Table 1. Suffixes for modern soils can be adapted to deeply buried palaeosols, but through a careful approach, as palaeosols can experience post-burial alterations (Fidolini and Andreetta, 2013).

Table 1 - Horizon suffixes used with soil horizon designations in the palaeosols described in the present guide.

Horizon suffix	Description
b	Buried soil horizon
c	Nodules or concretions
g	Gleying, redox accumulations, depletions, and mottles
k	Accumulation of pedogenic carbonates
p	Plough layer
ss	Pedogenic slickensides
t	Illuvial accumulation of clay

The first step in describing a palaeosol profile is the recognition of the horizons and their boundaries. Clues about pedogenic processes are also provided by other morphological characteristics within each horizon, which are summarised below.
Soil structure, intended as aggregates or peds, is a fundamental morphological expression, providing critical information about biologic and hydrologic processes. Soil aggregates are described in terms of shape (structural type), size (structural class), and strength (structural grade).

https://doi.org/10.3301/GFT.2023.04

Coatings, or cutans, are made of illuviated materials (clay, silt, organic material, or a variety of minerals) that accumulate on ped faces or pores and can provide evidence for illuviation and weathering processes linked to environmental, climatic, or drainage conditions.

Colours are assessed using the Munsell colour scale according to their hue, value, and chroma. Mottles areas within a soil horizon typically express as patches of oxidised (red-yellow) or reduced (grey-green) colours related to the iron dynamic. Mottling colours usually develop as the result of water saturation and correlate with the intensity and duration of redoximorphic conditions, generally resulting from alternating periods of saturation and drying.

For an extensive guide focused on palaeosols identification and classification, the reader can refer to Schoeneberger et al. (2012) and USDA-NRCS (2012).

DAYS 1 AND 2- THE PEDE APENNINE MARGIN

Geo-morphological setting

This external sector represents the morphological-structural junction between the uplifting chain and the subsiding Po Plain. In this area most of the tectonic units composing the Northern Apennines nappe pile crop out. In this guide, we aim to illustrate the recent evolution of the area and therefore we will concentrate on the Plio-Pleistocene units involved in deformation which account for the last deformation phases. However, the stratigraphy of these units is complex, considering the E-W lateral variations and the different names that have been used in the past. In Fig. 3b, three different successions for Quattro Castella area, Secchia Valley and Panaro Valley, have been reported. Above a Lower Pleistocene substratum made of light blue clays and yellowish sands at the top, the so-called Argille Azzurre formation (FAA) and Imola sands (IMO), respectively (Fig. 3b), an erosional unconformity delimits the base of the Emilia-Romagna Super-Synthem, which is divided into the Lower and Upper Emilia-Romagna synthems (AEI and AES, respectively; Fig. 3b). The AEI Synthem has a thickness varying from 30 to 150 m, an age interval between 820,000 and 478,000–424,000 years BP (Gunderson et al., 2014). The AES Synthem (424,000 years BP to Present) is up to 150 m thick and eight sub-synthems have been distinguished. Both Lower and Upper Emilia-Romagna Synthems are referred to the progradation of alluvial systems from the front of the chain to the distal plain during the Early Pleistocene-Recent (RER and ENI-AGIP, 1998; Pavesi 2008). The progradation is controlled by the tectonics in terms of uplift and migration of the buried thrust systems at the front of the chain which interfered with glacio-eustatic fluctuations of Middle and Late Pleistocene recorded by several transgressive-regressive cycles within the AEI and AES synthems (Amorosi, 2008).

To constrain the recent activity of tectonic structures, soil stratigraphy has been a very useful tool (e.g., Maestrelli et al., 2018; Zuffetti et al., 2018). Two main soil-stratigraphic units have been identified along the Northern Apennine margin (Maestrelli et al., 2018): an older deep, reddish soil is referred to as Collecchio palaeosol, is associated with either AES2 or AES3 subsynthems; a loess level, unconformably covering different surfaces, hosts a younger palaeosol (Ghiardo Soil, Cremaschi, 1987; Cremaschi et al., 2015).

Along the morphological transition between the plain and the hills is located the Pede-Apennine Thrust system (PAT; Maestrelli et al., 2018; Fig. 3). Different interpretations have been proposed for the PAT, spanning from the inferred activity of post-Middle Pleistocene major normal faults to high-angle normal faults due to the stretching associated to the crestal zone of the major anticlines connected to deep (> 15 km) blind thrust (Maestrelli et al., 2018 and references therein). Other authors consider the thrust faults and related folds belonging to the PAT system outcropping at places along the Emilia Pede-Apennine margin or in a slight external position (i.e., Stradella, Modena–Reggio Emilia and Bologna; Benedetti et al., 2003; Boccaletti et al., 2004; S. Colombano, Zuffetti and Bersezio, 2020). However, the PAT is an active thrust system with segments considered as SSW-dipping faults, dipping between 35°–70°. Moreover, following Vannoli et al. (2015), it can be considered a seismogenic source, with an associated expected maximum magnitude of 5.8–6.1.

https://doi.org/10.3301/GFT.2023.04

In these two first days, we will observe both the stratigraphic features of the Pede-Apennine margin along the Enza river section (Day 1) and the main characteristics of the recent and active tectonics of the PAT to which the developments of palaeosols are associated (Day 2).

https://doi.org/10.3301/GFT.2023.04

DAY 1 - ENZA RIVER

Stop 1.1 - Growth strata along the Enza River

Coordinates: Lat. 44°37’52.38”N, Long. 10°24’58.83”E

The Enza section (Fig. 5) provides a well-exposed transect across the Plio-Pleistocene, marine to continental, succession downstream of the PAT. Four stratigraphic-depositional intervals within the Lower Emilia-Romagna Synthem ($AEI_{a\text{-}d}$) have been recognised (Maestrelli et al., 2018). In agreement with Gunderson et al. (2014), the basal deposit (AEI_a) is represented by a greyish-greenish palustrine mudstone. This is unconformably overlain by AEI_b, made of clast-supported to chaotic, matrix-rich conglomerates, hinting at a transition from fluvial to mass-flow processes, topped by a greyish mudstone like the basal one. Within both AEI_a and AEI_b, it is possible to observe several, variedly preserved, palaeosols. Above, channelised conglomerates interbedded with floodplain mudstones mark the base of AEI_c and

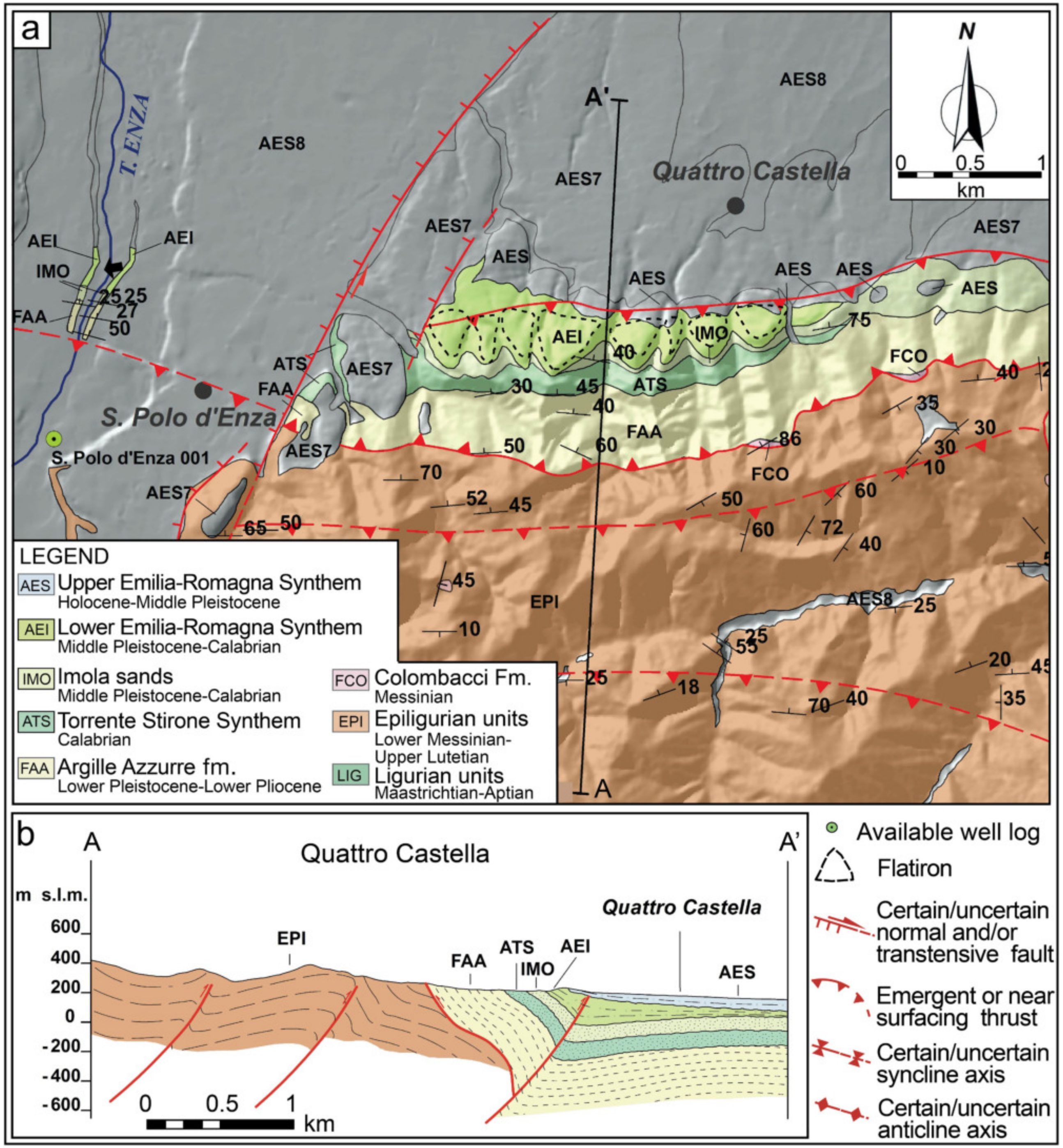

Fig. 5 - Map and cross-section depicting the geological setting occurring at the Quattro Castella Area. The Pede-Appenine Thrust (PAT) is responsible for the formation of the triangular facets occurring just South of the Quattro Castella town. NW of S. Polo d’Enza town, a buried sector of the PAT is responsible for the development of the growth fold nicely outcropping along the Enza River valley. Modified from Maestrelli et al. (2018).

https://doi.org/10.3301/GFT.2023.04

show evidence of a drainage axis transverse to the present Enza valley, thus sub-parallel to the PAT. Further up, AEI_c is dominated by a massive yellowish sandstone, grading into a mudstone, and recording the final infill and abandonment of the valley. Finally, a mass flow, matrix-rich and chaotic conglomerate, somewhat like the base of AEI_b, represents the uppermost AEI_d sub-unit. This latter deposit is intensely pedogenised and unconformably overlain by the Upper Emilia-Romagna Synthem (AES). Each depositional interval can be interpreted as a cycle of base-level variation, with coarse and fine deposits accumulating, respectively, at the end of a pulse of base-level lowering and during subsequent base-level rising. Mass-flow conglomerates record fluvial-footslope settings, fed from relatively steep and dominantly muddy slopes along the front, while mud-dominated, palustrine/floodplain settings hint at a depocenter along the Pede-Apennine front. Interestingly, the conglomerate fraction may have been reworked from older fluvial deposits that, for the lithostratigraphic constraint, would reasonably represent the feeder of the Imola Sands delta systems. The preservation of palaeosols within AEI_a and AEI_b shows how the deposition of these units was not accompanied by significant uplift or deformation, while both units were uplifted and deformed successively.

https://doi.org/10.3301/GFT.2023.04

DAY 2 - THE GHIARDO PLATEAU AND THE PEDE-APENNINE MARGIN

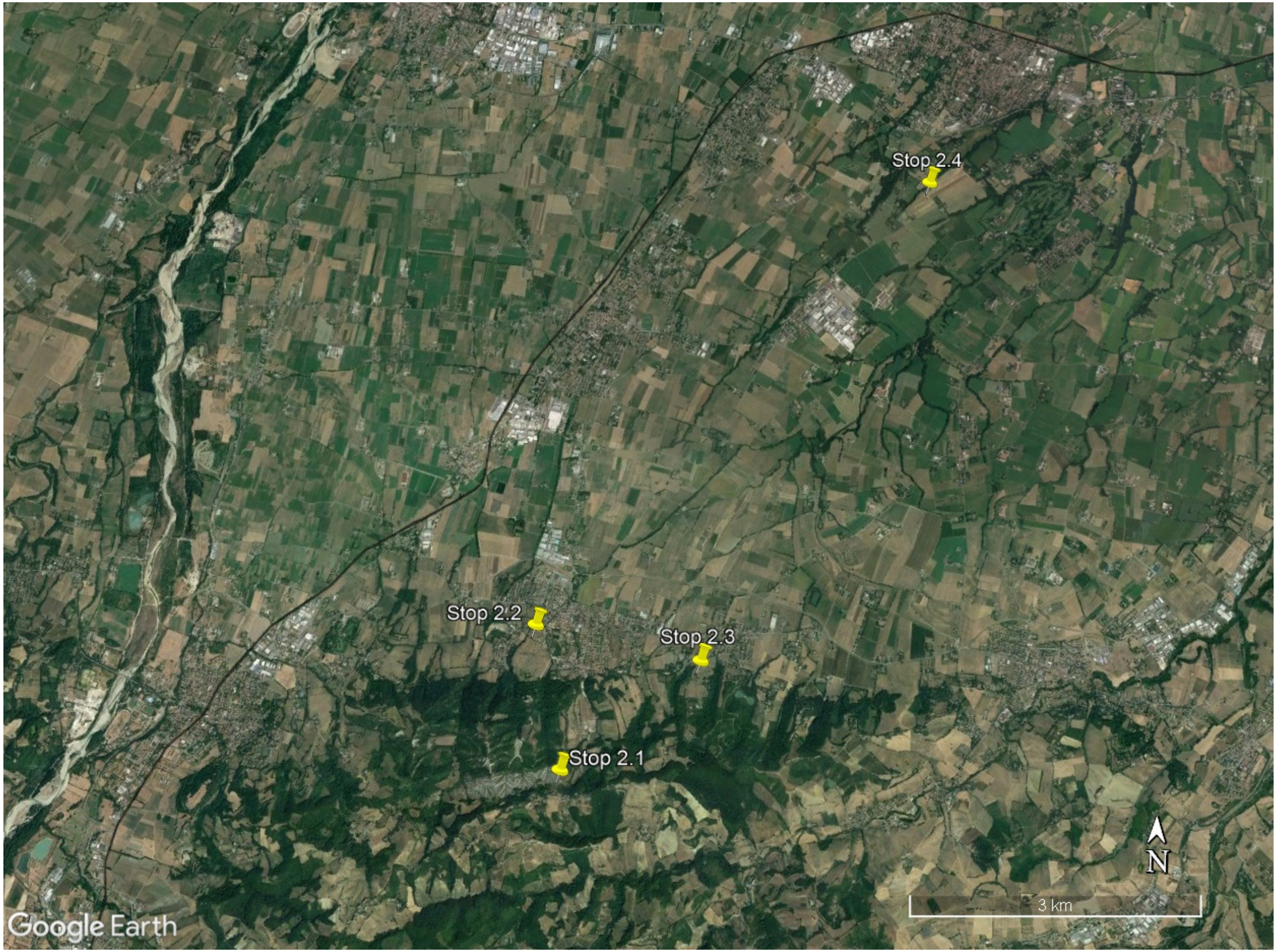

Fig. 6 - Google Earth view of the Day 2 itinerary with locations of the stops.

Stop 2.1 - Panoramic view along the road to Canossa – surface expression of the PAT

Coordinates: Lat. 44°37’13.28”N, Long: 10°28’21.97”E)

Moving South from Quattro Castella along the road to Canossa town, we crosscut the Apennine front, leaving back to the North the triangular facets generated by the recent activity of the Pede-Apennine Thrust (PAT). A few km south, climbing the Apennine hills, we will stop at a panoramic viewpoint showing the outcropping and deformed Quaternary deposits of the foothill (Figs. 6 and 7). From N to S, it is possible to observe the Lower-Middle Pleistocene fluvial deposits of the Lower Emilia-Romagna Synthem (AEI) overlaying the Lower Pleistocene coastal sandstones and conglomerates of the Imola Sands and Torrente Stirone Synthem. These deposits lay on the marine Pleistocene portion of the Argille Azzurre formation and are back-thrusted on top of Epiligurian deposits (EPI, Lower to Upper Miocene). The panorama clearly shows the back-thrusted forelimb of the anticline associated with the Pede-Appenine Thrust (PAT) as depicted in the geological cross-section of Figure 5b, highlighting the recent activity of this structure and suggesting its activity at least up ≈0.5 Ma (being this the upper temporal limit of the deformed AEI deposits in the area) (Maestrelli et al., 2018).

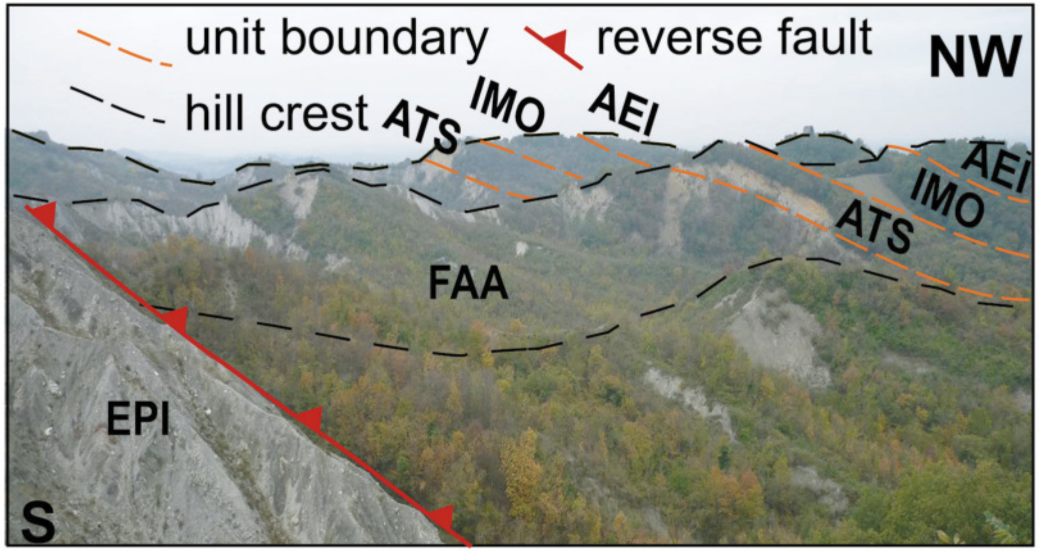

Fig. 7 - Panorama showing the outcropping stratigraphic sequence south of the Quattro Castella area, along the road to Canossa Town (modified from Maestrelli et al., 2018). The Pleistocene sequence, folded and tilted by the activity of the Pede-Apennine Thrust, is further deformed by the presence of a back-thrust associated with the PAT, pushing Pleistocene sediments on top of older (Lower to Upper Miocene) Epiligurian deposits (EPI). FAA: Argille Azzurre formation; ATS: Torrente Stirone Synthem; IMO: Imola sands; AEI: Lower Emilia-Romagna Synthem.

Stop 2.2 - Active thrusting at Quattro Castella

Coordinates: Lat. 44°38’1.48”N, Long. 10°28’5.13”E

A strong morpho-structural signature of active thrusting characterises the Quattro Castella area (Fig. 5a), where the Pede-Appenine Thrust (PAT) separates Upper Miocene-Lower Pliocene marine deposits from the Upper Pleistocene-Holocene alluvial deposits of the Po Plain. In this area, the thrust formed prominent faceted spurs (with a mean height of ~50m), a laterally continuous basal scarp, and strong fluvial erosion in the hanging-wall (Fig. 8a, b). Calculation of geomorphic indices of landforms and the slip rate of the structures also supports

https://doi.org/10.3301/GFT.2023.04

its recent activity (Boccaletti et al., 2004; Maestrelli et al., 2018). Pliocene and Pleistocene growth strata are well exposed in the creeks southwest of Quattro Castella and in the Enza Valley. The PAT at Quattro Castella is also responsible for the formation of an anticline, marked by a back-thrust that superposes the Pliocene FAA formation above the Epiligurian units, exposed at the anticline core (Barbacini et al., 2002; Maestrelli et al., 2018) (well visible at Stop 2.1, Fig. 6). This suggests the important role played by the intercutaneous tectonics in the deformation style of the Pede-Apennine margin. In this sector, the PAT has been interpreted as a thrust dipping at 40° or more (Bonini, 2013), as supported by the seismic lines analysis (Maestrelli et al., 2018), showing a clear syntectonic wedging of Pliocene-Quaternary sediments associated with the PAT activity. In addition, these sediments show thinning and tilting produced by the lifting of the back limb of a more external thrust anticline, which has also (likely) lifted the Ghiardo Plateau (Stop 2.3; Figs. 9 and 10). This fold represents an important ramp anticline ahead of the PAT, and extends south-eastward up to Scandiano and Casalgrande towns, whereas toward the northwest it is interrupted by a NE-SW oriented fault system passing through Bibbiano and Ghiardo and down-throwing their western blocks. Both normal faults appear to be active, showing geomorphic features allowing their

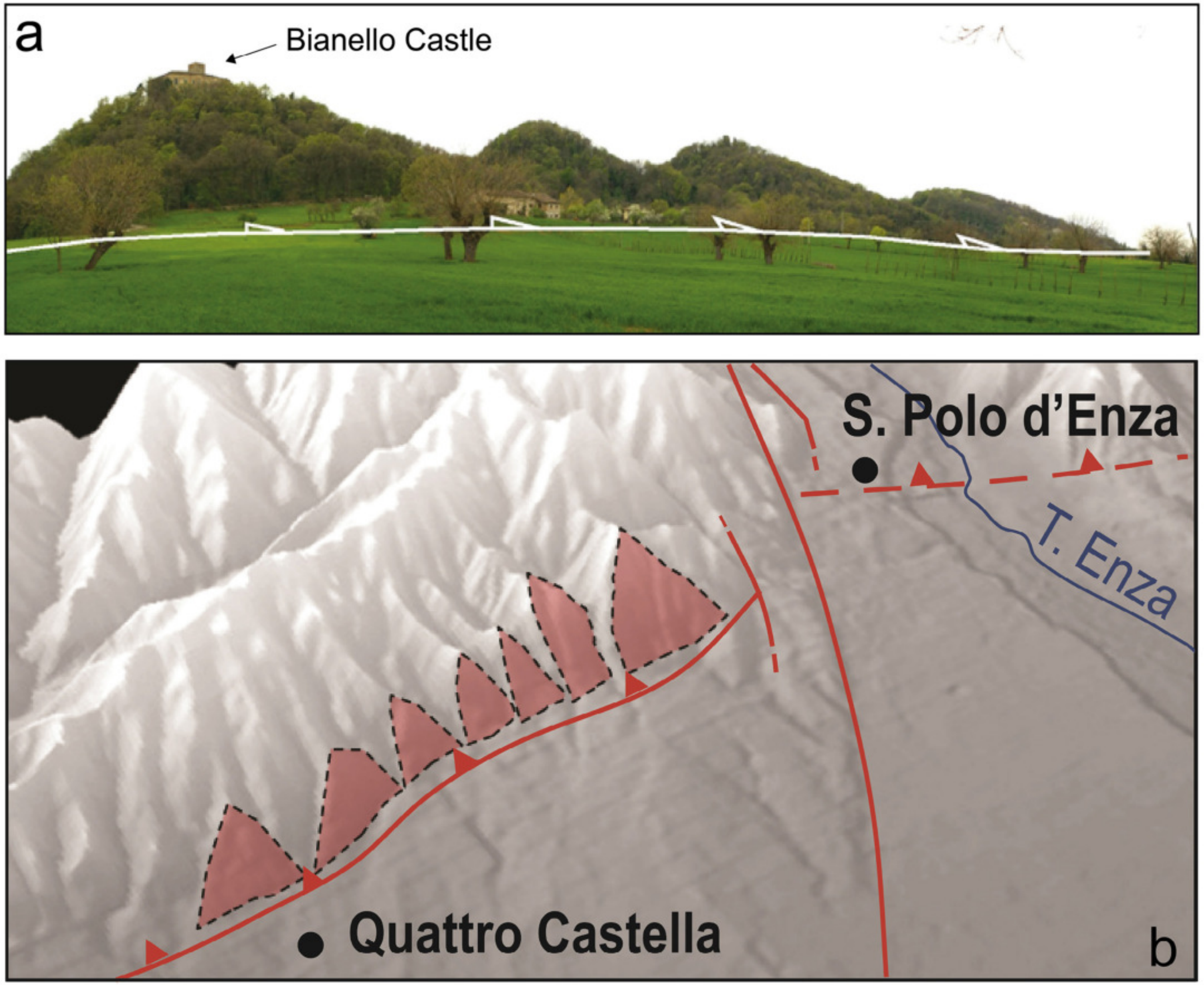

Fig. 8 - Morpho-structural characteristics at the surfacing of the active Pede-Apennine Thrust front at Quattro Castella, generating triangular facets. a) Triangular facets just south of Quattro Castella. The Bianello Castel is indicated for scale. b) DEM of the Quattro Castella area with its structural and morphological interpretation.

https://doi.org/10.3301/GFT.2023.04

identification as roughly sub-vertical tectonic scarps (see Castiglioni et al., 1997, 2001; Boccaletti et al., 2004, 2011). Their tectonic nature is visible in that they interrupt the PAT toward the west, and break off the Montecchio anticline (west of our study area) from the Ghiardo anticline. These structures represent the north-western boundary of the Ghiardo anticline and are characterised by an important left-lateral component of displacement (Figs. 8,10).

Stop 2.3 - Panoramic view of the Ghiardo Plateau

Coordinates: Lat. 44°37'50.77"N, Long. 10°29'25.02"E

Stop 2.3, standing on the foothill of the Apennine margin, will show us a panoramic view of the Ghiardo Plateau (Fig. 9), (which will be the focus of Stop 2.4). The stop is located in correspondence of the morphological rupture associated with the PAT, from which splays a secondary, and more external, thrust responsible for the uplift and deformation of the Ghiardo Plateau. Looking carefully, it is possible to observe a gentle syncline depression located among the foothill and the morphological high corresponding to the present-day Ghiardo town area. This morphological depression represents a structural syncline, resulting from the coupled deformation effect of the main PAT and its splay, and acted as a depocenter for sediments up to historical time, when Romans drained out this palustrine setting, modifying the environment. Upper Pleistocene sediments are also identified in the depression and are correlated with sediments and palaeosols making up the top of the Ghiardo Plateau (Carnicelli et al., 2003). Their stratigraphy and implications will be the focus of Stop 2.4.

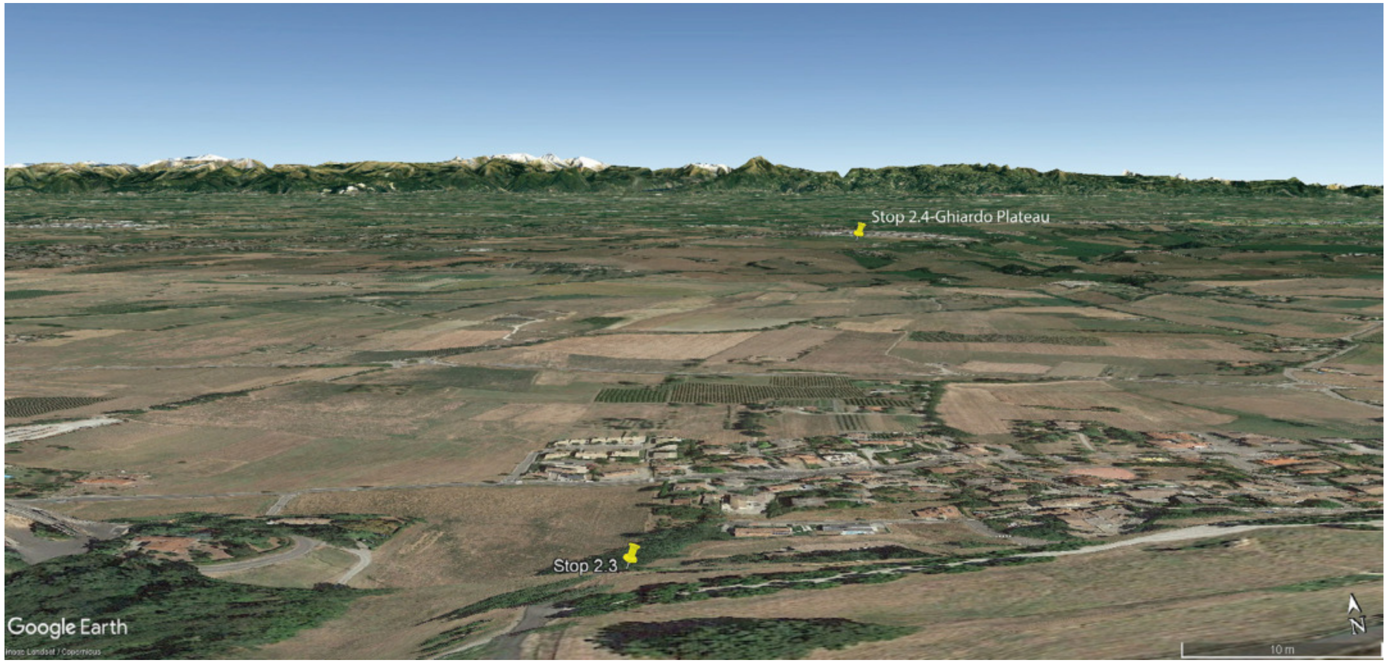

Fig. 9 - Panorama (Google Earth) of the Ghiardo Plateau seen from Stop 2.3, with the Po plain and the Alps in the background.

https://doi.org/10.3301/GFT.2023.04

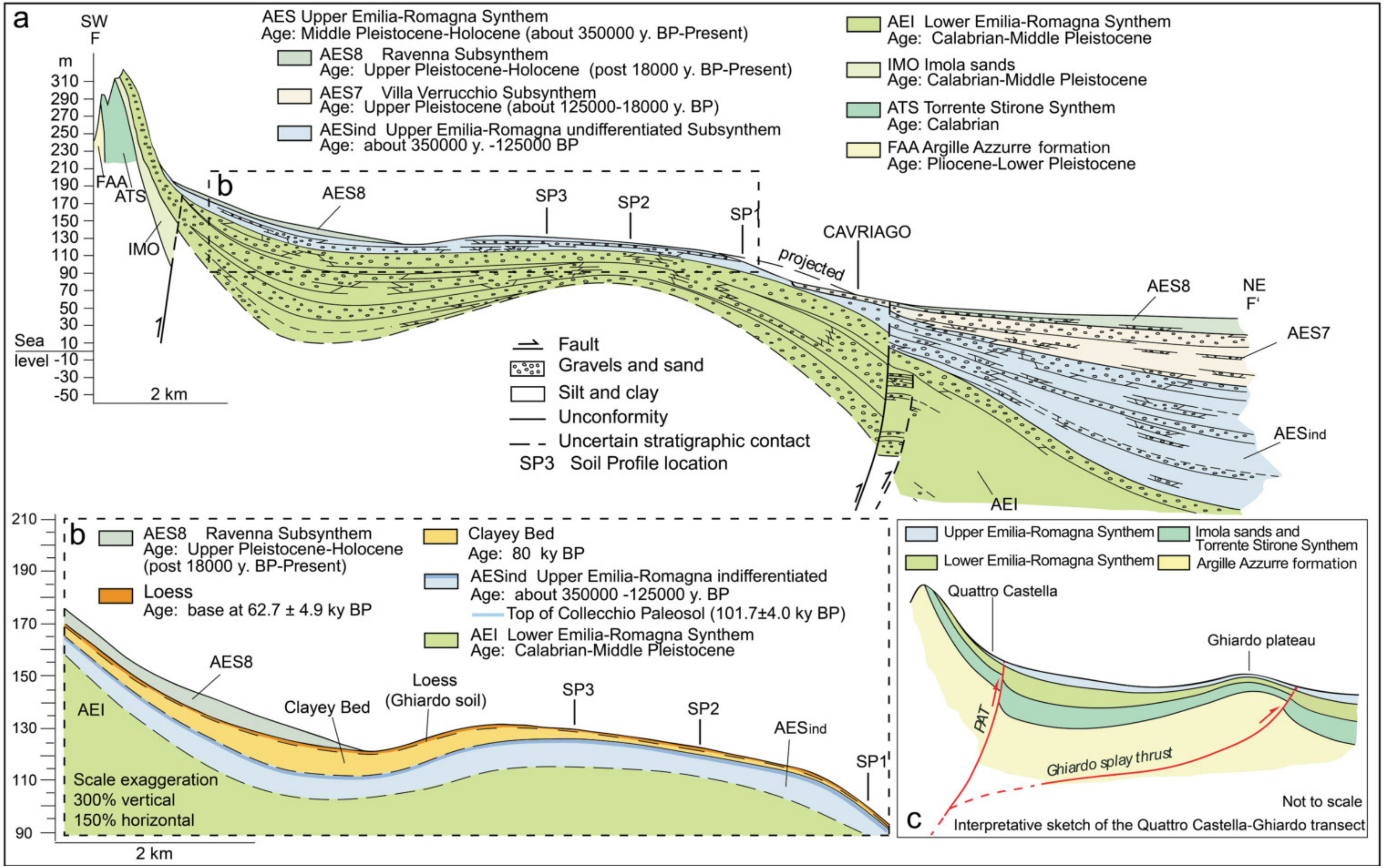

Fig. 10 - (a) Superficial geological section crossing the Ghiardo plateau (trace location is visible in Figure 3) (modified from Carnicelli et al., 2003 and Maestrelli et. 2018). (b) Vertically exaggerated close-up showing the internal geometry of the superficial units present in the Ghiardo area. Thicknesses are derived from soil profile analysis and well data (https://applicazioni.regione.emilia-romagna.it/cartografia_sgss/user/viewer.jsp?service=geologia). Syncline geometry with increasing thickness of the clayey bed is clearly shown in this section. (c) Interpretative and not to scale sketch of the Ghiardo plateau structural setting.

Stop 2.4 - Palaeosols of the Ghiardo Plateau

Coordinates: Lat. 44° 40’ 46.16”N, Long. 10° 31’ 12.27”E

The pedological data refer to the area in front of the Quattro Castella Mountain front, known as Ghiardo Plateau (Figs. 3, 9). This plateau rises gently northwards from a depression placed north of the Quattro Castella flatirons (Figs. 5, 7, 8) to elevations as high as up to 135 m above sea level, then descending more steeply on the northern edge (Fig. 10). This landform is interpreted as the surface expression of an anticline, connected at depth with a splay thrust emanated from the PAT (Fig. 10c). A small basin, with axis parallel to the margin, formed in the syncline between the PAT and the external anticline, and is known to have been a palustrine setting and to have been reclaimed in Roman times. Upper Pleistocene sediments making up the top of the plateau are identified as belonging to undifferentiated AES (AESind in Figs. 10, 11), while very recent units are reported in the syncline (Carnicelli et al., 2003, Pizziolo et al., 2016; Fig. 10).

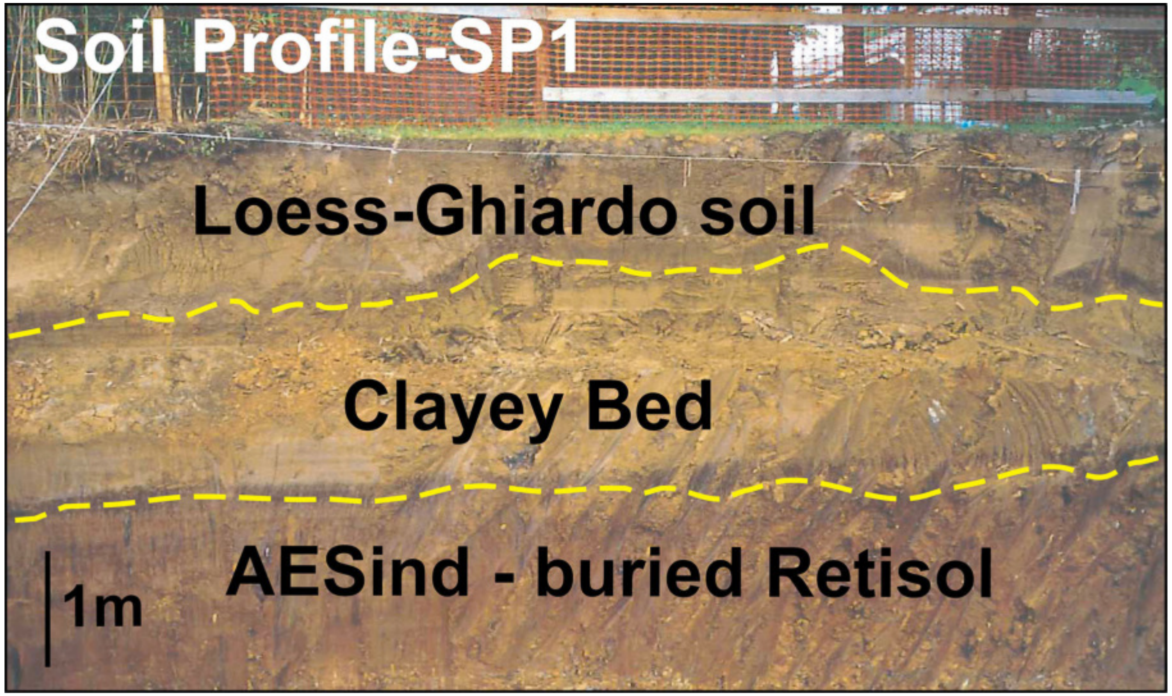

Fig. 11 - Overall view of the succession of palaeosols and pedosediments outcropping on the southern slope of Ghiardo Plateau; at the base, the reddish palaeosol (in this outcrop showing not much of Retic properties); on top of it, the yellow clay bed with palaeosol characters and, on top, the surface soil, developed on loess deposits (modified from Maestrelli et al., 2018).

In this area, the Ghiardo soil, developed on a thin (≈2 m) loess cover, is found above a yellow clay body. A characteristic “mukkara” surface (Fig. 12, Schaetzl and Thompson, 2015) marks the loess-clay boundary and is the site of Palaeolithic findings (Cremaschi et al., 2015). The presence of a deeper buried, more developed, palaeosol was reported in Cremaschi (1987); in the last revision (Cremaschi et al., 2015) the yellow clay body is interpreted as heteropic with the AES sediments and the Collecchio palaeosol.

Our reference for the interpretation of the Ghiardo Plateau soil and “shallow sediments” stratigraphy is a combined soil profile and borehole in site SP2 (Fig. 13; 44° 40’ 45” N, 10° 31’ 12” E; see Fig. 10a,b for location). In the soil profile (Table 2), we observed, from bottom upwards:

a) a deep palaeosol developed on a shallow silty cover and, mostly, on a major gravel body observed in the borehole. The palaeosol shows strongly developed clay translocation, Retic features (IUSS Working Group WRB, 2015) and reddish (7.5YR) colour. The gravels, coming

https://doi.org/10.3301/GFT.2023.04

from calcareous formations, are fully decalcified and extensively shattered down to about 3 m below the top of the buried palaeosol. Clay mineralogy is marked by transformation minerals, such as vermiculite/smectite and illite/smectite mixed layers; the absence of hydroxyl-Al interlayers is significant, suggesting that this soil never underwent prolonged acidification.

b) A shallow (50-100 cm) yellow clay body, showing Vertic soil features and extensive secondary carbonate accumulation, upper-bounded by the “mukkara” surface (Cremaschi et al., 2015, Figs. 11, 12, 13).

c) The surface soil, about 1.5 m thick, developed onto the loess level. It is very silty, with well-developed clay illuviation, and it is carbonate-free but fully base-saturated (Fig. 13; Table 3).

These observations are easily correlated with published data (Cremaschi, 1987; Cremaschi et al., 2015). The deeply buried palaeosol is referred to a palaeosol extensively outcropping to the west, on the same AES synthem; it can be traced for a short distance to the south, before it gets too deep, and marks the top surface of unit AESind. The clay body increases its thickness southwards, to the sites described by Cremaschi (1987) and Cremaschi et al. (2015) and to site SP3 (Fig. 12, see Fig. 10a,b for location); it cannot then be considered as heteropic with the AESind, as it lies on top of it. It is instead interpreted here as a continuous bed lying above the major unconformity represented by the Collecchio palaeosol. The surface soil is extensively mapped in the area as the Ghiardo soil.

OSL dating of profile SP2 (Fig. 13) yielded the following results:

- Base of the loess (about 70 cm depth): 62.7 ± 4.9 ky (OSL1 in Fig. 13).
- Clay bed: 120.1 ± 7.0 ky (OSL2 in Fig. 13).
- Top of the palaeosol: 101.7 ± 4.0 ky (OSL3 in Fig. 13).

There is a clear inconsistency between OSL2 and OSL3. The main possible source of the inconsistency is the change in the radioactive background with time. Carbonate translocation is quite active in this outcrop, concretions being present both within the clay layer and on the top part of the palaeosol, where they have a clear post-burial origin. As the surface loess cover was a major carbonate source, at least part of the carbonates in the clay layer could also be post-burial. Carbonate accumulation can cause either increases or decreases of radioactive dose, due respectively to uranium enrichment and

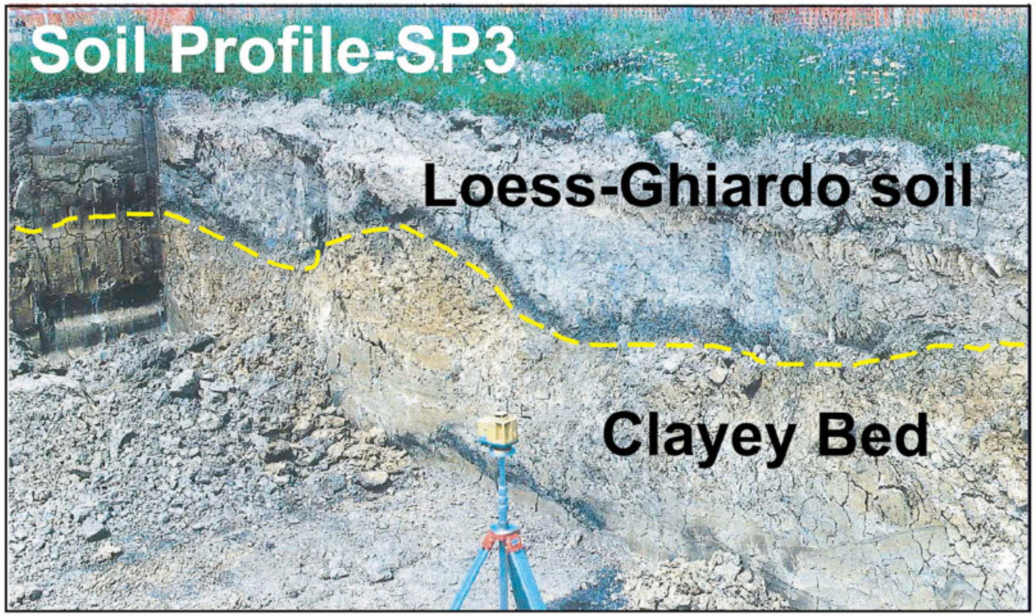

Fig. 12 - Detailed view of the upper part of the palaeosol-sediment succession, showing to advantage the “mukkara” surface separating the yellow clays from the soil on loess (modified from Maestrelli et al., 2018).

https://doi.org/10.3301/GFT.2023.04

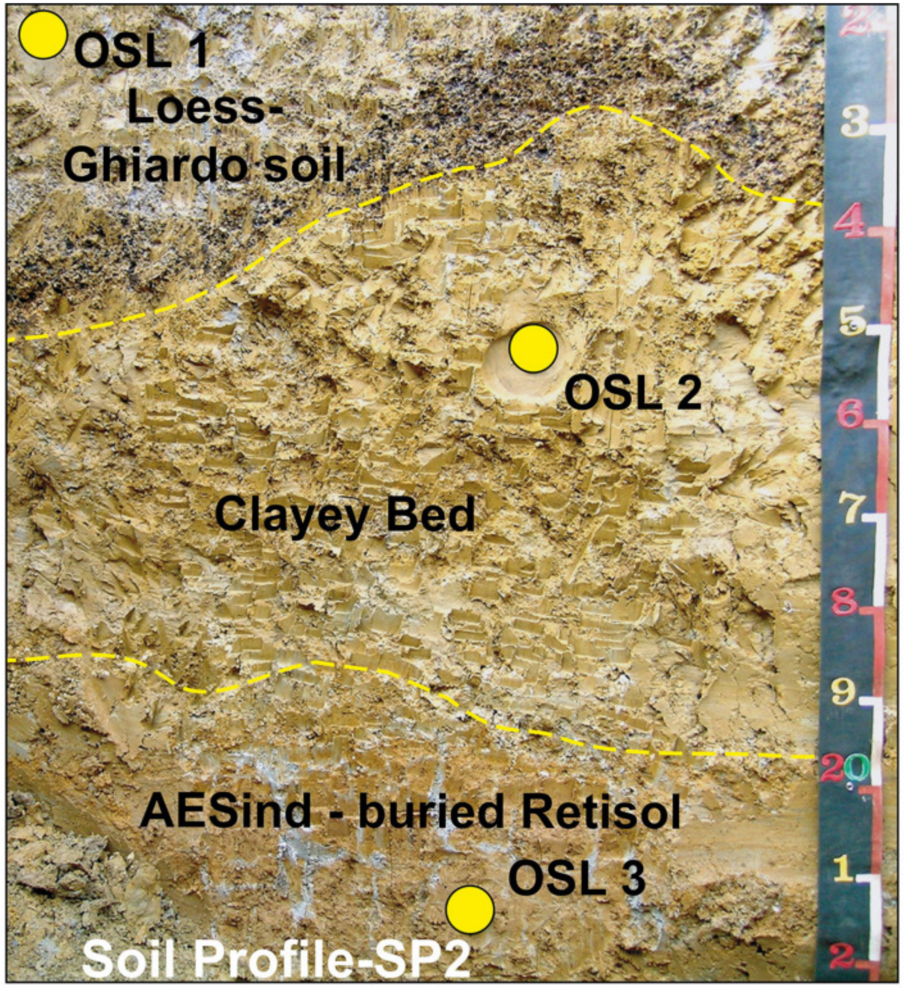

Fig. 13 - Detail of the lower part of the succession, seen in the original soil profile and showing the positions of the samples taken for OSL dating (modified from Maestrelli et al., 2018).

dilution of the silicate matrix. Recently, Cremaschi et al. (2015) produced a more reliable dating of the yellow clay body, placing the top of it at 81.6 ± 10.9 ky (Cremaschi et al., 2015). This comes with various further dates from the base of the loess cover, in full agreement with our results and those of Martini et al. (2001), firmly constraining it to 60-70 ky.

The buried Collecchio palaeosol records a major soil-forming episode, lasting a minimum of some tens of thousands of years (Carnicelli and Costantini, 2013; Carnicelli et al., 2015), on a stable geomorphic surface with a deep-water table. In other words, it records a terraced landform, by-passed by rivers, and elevated with respect to the active alluvial plain. This palaeosol marks a high-rank unconformity, recognised at sub-synthem level as marking the top of either AES3 sub-synthem or AESind unit (Carnicelli et al., 2003 and references therein).

The peculiarity of the Ghiardo Plateau is the presence of the yellow clay level on top of the Collecchio palaeosol. The yellow clays are pedogenised, but to quite a low degree; they then record a later and lesser pedogenesis, and can only be interpreted as a sedimentary body, separated from AESind by a major unconformity. The nature of the clays rules out both aeolian and volcanic sources; clay content is much too high for aeolian deposits, while pedological characters rule out massive weathering of either loess or tephra into clay. The yellow clay level was then deposited by water transport. Such a depositional event, on top of a long-standing terraced surface, requires a major, and unusual, base-level change, bringing a fluvial terrace back to the status of depositional area.

A strong similarity exists between the yellow clay body and soils on the outcropping AEI deposits near Quattro Castella, which are, therefore, a likely sediment source. The formation of this sedimentary bed can be related to a phase of strong uplift of the PAT, triggering high-rate erosion and sediment supply. Strong uplift of the PAT, with the development of a high-lying hilly relief a few kilometres upslope, is also the only mechanism that can be considered for the base level change involving the ancient river terrace. On the other hand, as shown in Fig. 10b, the yellow clay level was significantly deformed after the end of its deposition, at about 80 ky by the development of the anticline. In our opinion such a

https://doi.org/10.3301/GFT.2023.04

deformation stopped the deposition of this layer, indicating that, after 80 ky, the uplift rate of the anticline structure might have exceeded that of the main PAT.

Table 2 - Soil profile description.

Horizon	Depth (cm)	Description
Ap1	0-25	Medium, moderate cloddy structure; moist colour 10YR 4/2; friable when moist, slightly plastic; silt loam; non-calcareous; gradual, smooth boundary to:
Ap2	25-40	Medium, moderate blocky subangular structure; moist colour 10YR 5/4; friable when moist, slightly plastic; silt loam; few non-cemented FeMn masses, few FeMn coatings; non-calcareous; gradual, smooth boundary to:
Btg1	40-60/70	Strong, medium angular blocky structure; moist colour 10YR 4/2, 40% oximorphic masses, 3-4 mm, 7.5YR 5/8; friable when moist, slightly plastic; silt loam; occasional clay and silt coatings; common cemented FeMn masses, 1 mm; few non-cemented FeMn masses, 3-4 mm; non-calcareous; diffuse boundary to:
Btg2	60/70-85/115	Moderate, fine prismatic structure; moist colour 10YR 5/4; vertical reductimorphic streaks, 10YR 5/1, 2-5 mm wide, 40% of surface; silt loam; discontinuous clay coating in streaks, occasional elsewhere; common non-cemented FeMn masses; few cemented FeMn masses; non-calcareous; clear wavy boundary to:
Bc	85/115-100/135	Structureless firm; moist colour 10YR 5/4; 50% cemented FeMn masses, up to 10 mm diameter; non-calcareous; abrupt wavy boundary to:
2Bssb	100/135-145/155	Weak, medium, angular blocky structure; moist colour 10YR 5/6; pockets of 10YR6/1 in the upper part; extremely plastic and adhesive; silty clay; continuous pressure faces; intersecting slickensides; few to common FeMn cemented masses, <1 mm; slightly calcareous; diffuse boundary to:
2Bkssb	145/155-170/190	Weak, medium, angular blocky structure; moist colour 10YR 5/6; broad, faint streaks 10YR 6/1; extremely plastic and adhesive; silty clay; continuous pressure faces; intersecting slickensides; common carbonate masses, both cemented and non-cemented, abundant at lower boundary; few to common FeMn cemented masses, <1 mm; mass slightly calcareous; abrupt, smooth boundary to:
3Btgb	170/190-225	Moderate, fine blocky angular structure; moist colour 7.5YR 4/6; reticulated streaks, 10YR 6/1; moist friable, highly plastic, non adhesive; silty loam; discontinuous clay coatings on ped faces, 7.5YR 4/2 or 4/4; FeMn coatings and cemented masses within streaks; non-calcareous.
3Bcb	225+	On the bottom of the profile, more than 40% cemented FeMn masses, size up to 5 mm.

Table 3 - Soil analysis

Horizon	Depth (cm)	pH, H_2O	Organic C (%)	CaCO3 tot (%)	Clay (%)	Silt (%)	Sand (%)	Coarse sand (%)	Medium/fine sand (%)	Very fine sand (%)	C.E.C. ($cmolc^+/kg$)
Ap_1	0-25	7.5	1.3	0	18.0	77.0	5.0	3.0	1.0	1.0	17.5
Ap_2	25-40	7.5	0.4	0	35.0	61.0	4.0	1.0	1.0	2.0	22.6
Btg_1	40-70	7.3	0.6	0	34.0	59.0	7.0	2.0	1.0	4.0	25.1
Btg_2	65-115	7.3	0.3	0	37.0	56.0	7.0	3.0	1.0	3.0	25.3
2Bssb	100-150	7.2	0.2	0	57.0	37.0	6.0	0.0	0.0	6.0	35.1
2Bkssb	150-170	7.4	0.2	0	60.0	39.0	1.0	0.0	0.0	1.0	33.9
3Btgb	190-225	7.5	0.2	0	32.0	63.0	5.0	1.0	1.0	3.0	20.0

DAY 3 - THE PLIO-PLEISTOCENE INTERMONTANE MUGELLO BASIN

Fig. 14 - 3D view of the Mugello Basin looking from to the North with location of the two stops, from Google Earth.

https://doi.org/10.3301/GFT.2023.04

Geo-morphological setting

The Mugello Basin (Fig. 14), located ca. 30 km north of Florence, is one of the intermontane (or peripheral *sensu* Martini and Sagri 1993) basins developed on the western flank of the Northern Apennines (Figs. 2 and 15) and filled with Upper Pliocene-Pleistocene alluvial and lacustrine deposits.

The basin (Fig. 16) has a WNW-ESE structural trend with a length of 25 km and width of 15 km, being drained by the Sieve River, one of the most important Arno River tributaries. The internal basin's hydrography is characterised by a dense network of small tributaries of the Sieve River descending from the basin's margins.

The Mugello basin fill

The infilling of the basin occurred in a fluvio-lacustrine phase followed by an alluvial phase (Benvenuti 1997; 2003). During the early fluvio-lacustrine phase (Late Pliocene?-Early Pleistocene), the Mugello Basin had an internal drainage, with peat and silty clay up to 100 m thick accumulated in a palustrine environment in the western part of the basin (Barberino di Mugello area) and more than 600 m of sediment accumulated in its strongly subsiding southern part (Borgo S. Lorenzo area). This thicker succession (referred to as

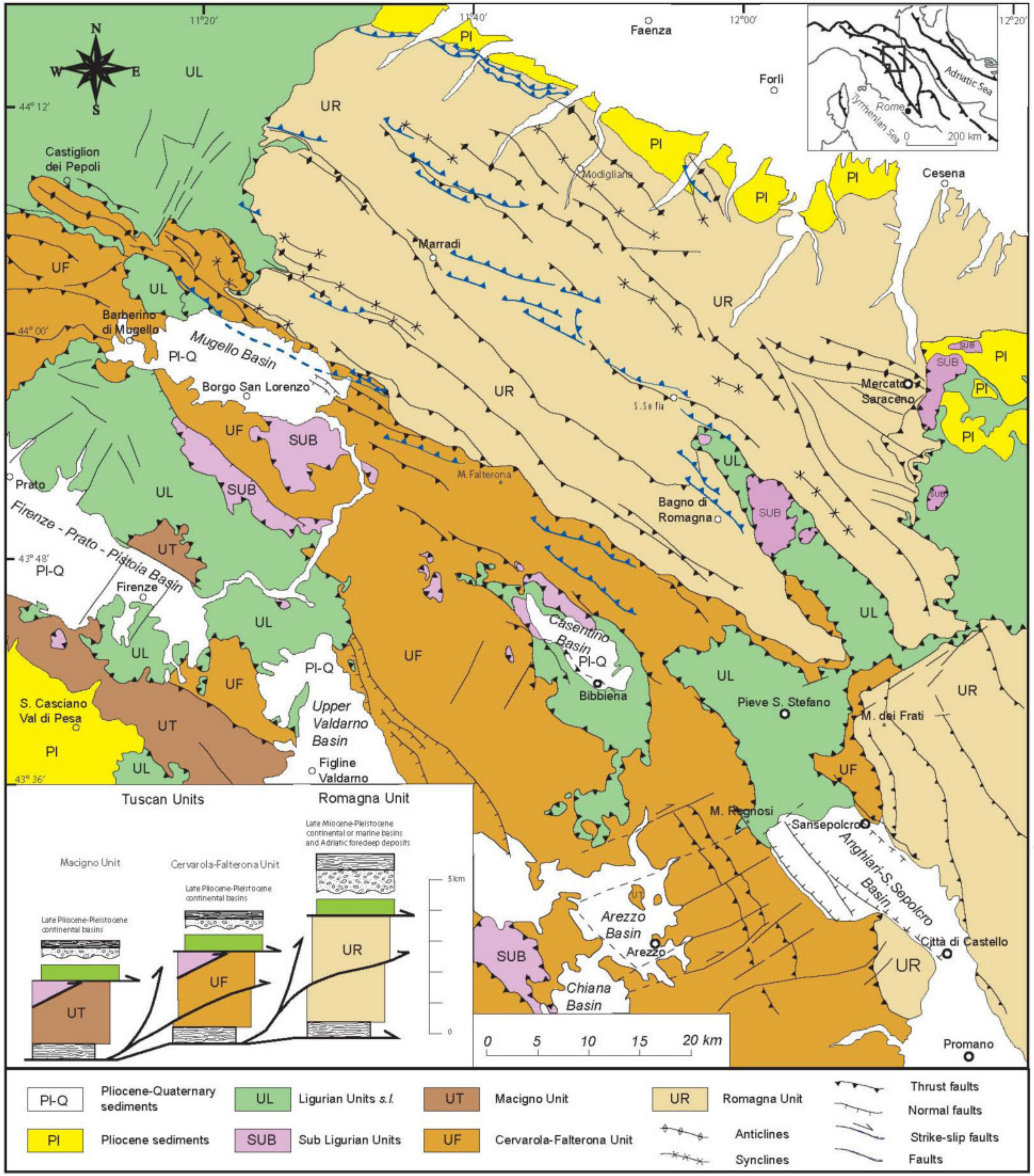

Fig. 15 - The main structural features of the outer portion of the Northern Apennines (after Sani et al., 2009a).

https://doi.org/10.3301/GFT.2023.04

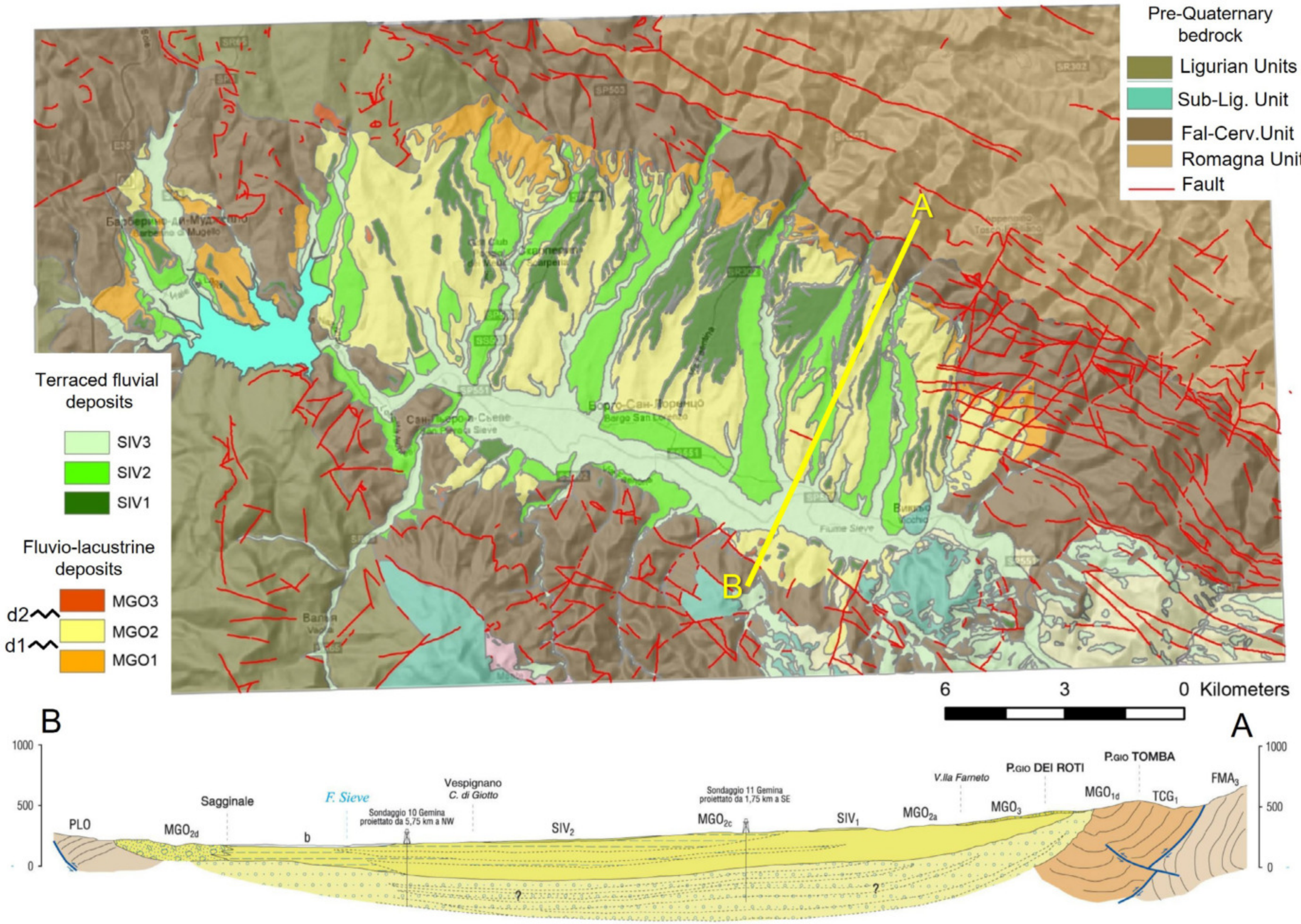

Fig. 16 -The Mugello Basin: simplified geological map and sections (modified from Sani et al., 2009a and Bortolotti et al., 2015). Mugello synthem (MGO): Ronta sub-synthem (MGO1); Pulicciano sub-synthem (MGO2); Farneta sub-synthem (MGO3). Sieve River synthem (SIV): Scarperia sub-synthem (SIV1); Luco di Mugello sub-synthem (SIV2); Sagginale sub-synthem (SIV3).

Mugello synthem, MGO) consists of a basal wedge of alluvial gravel and sand, ca. 20 m thick, detected only by cores (Gemina, 1962), overlain by lacustrine silty clay intercalated with lignite lenses and interfingered with fan-deltaic gravel and sand. The sediment dispersal during the fluvio-lacustrine phase was persistently from the NE toward the basin axis, as indicated by gravel imbrication and other palaeocurrent indices in fan-delta deposits. The development of fan deltas (Benvenuti, 1997; 2003) at the northern margin was strongly affected by syn-depositional uplift and tilting of this shoulder, forced by the reactivation of compressional structures (Sani et al., 2009a), as testified by pinching-out of deposits and occurrence of angular and progressive unconformities (*sensu* Riba, 1976).

Fan-delta strata are generally dipping toward the SSW, but the inclination ranges from vertical, locally overturned, in the oldest strata to 10° in the youngest ones. The transition from the steeper- to gentler-inclined strata varies from gradual to unconformable angular, with two major unconformities d1 and d2 (Fig. 17). Unconformity d1 separates the lower fan-delta system (Ronta sub-synthem, MGO1) from the upper fan-delta system (Pulicciano sub-synthem, MGO2), whereas unconformity d2 separates these fan-deltaic deposits from the alluvial-fan deposits closing the first phase of basin filling (Farneta sub-synthem, MGO3). These depositional systems show an alternation of alluvial-fan, fan delta-front, lacustrine, and floodplain facies associations (Benvenuti, 2003). The alluvial facies indicate sediment dispersal by flashy, hyper-concentrated flows in the form of sheet floods and moderately channelised flows. Deposits of the former predominate in the LFD system and deposits of the latter in the UFD system and this change is attributed to the greater volumes of water yielded by enlarged fan catchments (Benvenuti, 2003). The fan deltas are mostly shoal-water type with subordinate Gilbert-type deltas, indicating predominant shallow water depths at the lake margin. The

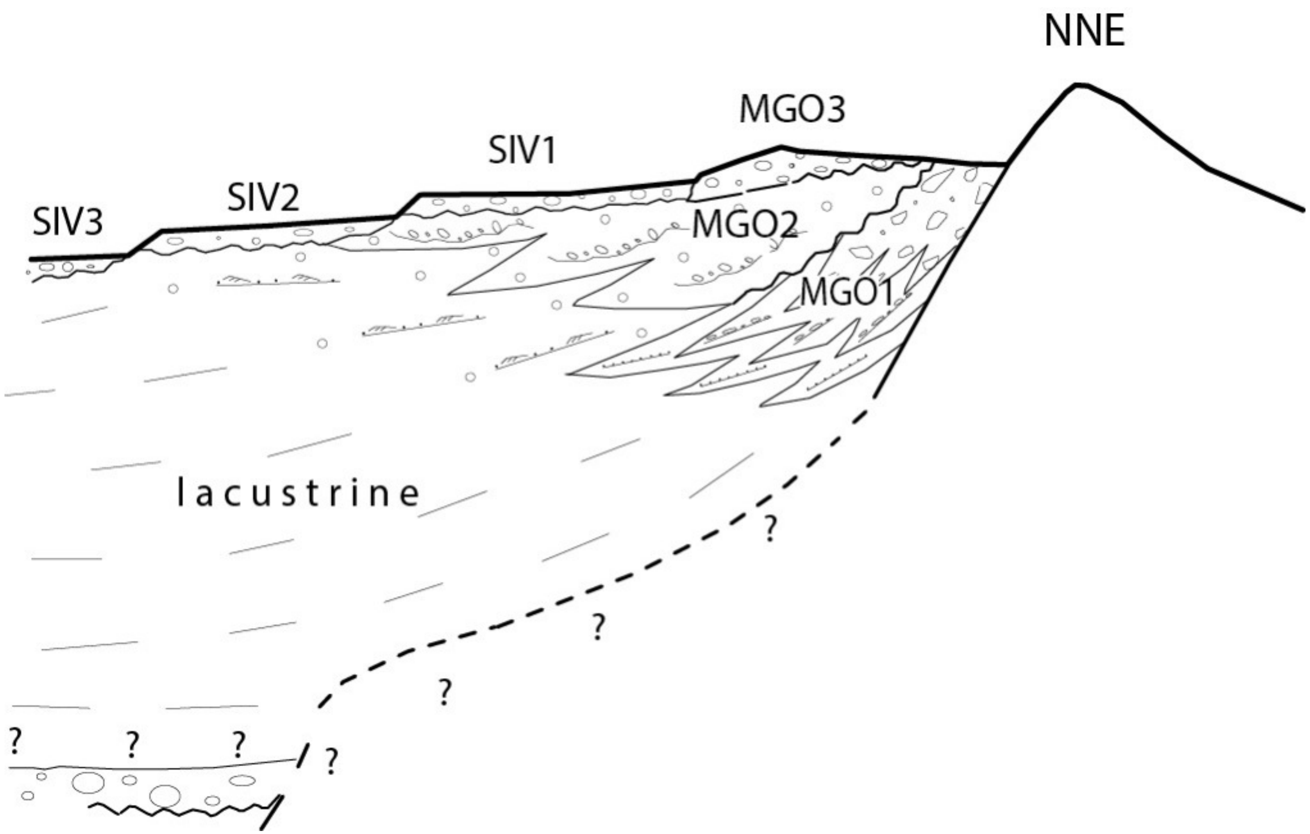

Fig. 17 - Schematic representation of the syntectonic wedge of fluvio-lacustrine deposits along the NE margin of the basin. Mugello Synthem (MGO): Ronta sub-synthem (MGO1); Pulicciano sub-synthem (MGO2); Farneta sub-synthem (MGO3). Sieve River Synthem (SIV): Scarperia sub-synthem (SIV1); Luco di Mugello sub-synthem (SIV2); Sagginale sub-synthem (SIV3).

https://doi.org/10.3301/GFT.2023.04

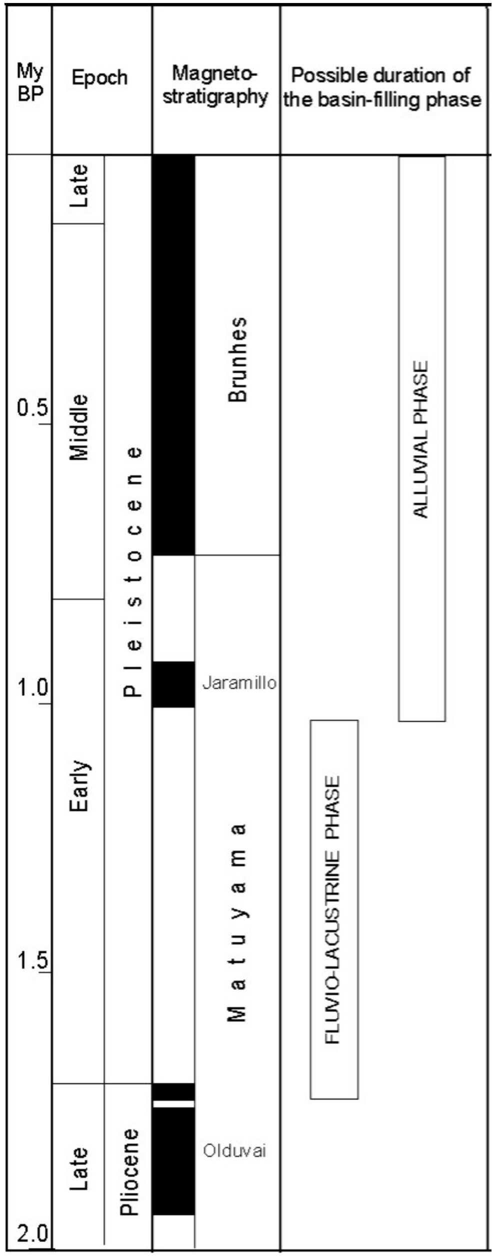

Fig. 18 - Chronological constraints for the Mugello succession (see Abbazzi et al., 1995 for details)

topmost MGO3 deposits are preserved only in their gravelly alluvial-fan portion and are deeply weathered as indicated by the palaeosol to be examined at Stop 3.1.

The chronostratigraphic extent of the fluvio-lacustrine phase has been established on the basis of terrestrial vertebrate fauna (Fig. 18; Abbazzi et al., 1995), and although it corresponds mostly to the Early Pleistocene with a possible initiation in the Late Pliocene, an epoch of significant climatic changes related to glacial-interglacial fluctuations, the sparse pollen flora in the basin suggests that the climate was nearly warm-temperate, characterised by minor fluctuations in both air temperature and ground moisture (Sanesi, 1965).

During the subsequent alluvial phase (latest Early Pleistocene?-Holocene), three major episodes of base-level fall occurred, resulting in a distinctly terraced alluvial succession, the Sieve River synthem SIV, articulated into three sub-synthems: Scarperia sub-synthem (SIV1), Luco di Mugello sub-synthem (SIV2), and Sagginale sub-synthem (SIV3). These sediments are made of variably pedogenised gravel, sand, and mud (Sanesi, 1965). Soils and palaeosols (on SIV1) found on the succession clearly show the relative temporal succession of the surfaces.

Stop 3.1 - Palaeosols on the highest terrace of the Mugello basin

Coordinates: Lat. 44° 0’2.39”N, Long. 11°17’59.36”E

The stop allows to observe the palaeosol (Fig. 19; Table 4) partly preserved on the surface of MGO3 unit.

This soil formed on alluvial deposits of the said unit, though there is, here too, a doubt about aeolian contribution, suggested by the silt content, which is high with respect to the other indicators of the degree of weathering.

Deep weathering is indicated by the status of the coarse fragments, by the low base saturation and by the low clay activity, which is always <0.5.

The clay mineral assemblage is dominated by hydroxy-interlayered 2:1 minerals; though these data are old, it is possible to infer a high degree of Al-interstratification; kaolinite is also present in significant amounts. This is a type of clay mineral assemblage that is commonly considered typical of Alisols formed in subtropical moist climates.

Overall, this soil appears to belong to a different, older, palaeosol generation with respect to the palaeosol examined in the previous day; stratigraphic position supports a Middle Pleistocene age. This should be actually considered as a maximum age; observation will show that there are doubts about profile

https://doi.org/10.3301/GFT.2023.04

Table 4 - Soil profile description

Horizon	Depth (cm)	Description
A	0-12	Fine, moderate blocky subangular structure, friable; dry colour 5YR 4/8; loam, few <3 mm coarse fragments, strongly weathered; common small FeMn cemented masses; clear, wavy boundary to:
AB	12-42	Weak, fine, angular blocky structure, friable; dry colour 5YR 3/6; clay loam; few <3 mm coarse fragments, strongly weathered; reductimorphic areas, 7.5YR 3/1; common small FeMn cemented masses; clear, wavy boundary to:
2Bt1	42-120	Moderate, medium, angular blocky structure, firm; moist colour 2.5YR 4/6; clay; few <3 mm coarse fragments, strongly weathered; discontinuous clay coatings on ped faces; discontinuous FeMn coatings; common small FeMn cemented masses; gradual, wavy boundary to:
2Bt2	120-180+	Moderate, medium, angular blocky structure, firm; moist colour 5YR 4/6; clay; few <3 mm coarse fragments, medium weathered; discontinuous clay coatings on ped faces; discontinuous FeMn coatings; few small FeMn cemented masses; unknown boundary

Table 5. Soil chemical and physical properties of the "Suolo Mercatale Battistini"

Horizon	Depth (cm)	pH, H_2O	OC (%)	CaCO3 tot (%)	Clay (%)	Silt (%)	Sand (%)	Base sat. (%)	C.E.C. (cmolc$^+$/kg)
A	0-12	4.8	2.9		24.6	36.3	39.1	18.4	16.9
AB	12-42	4.9	0.7		33.5	40.9	25.6	16.6	14.4
$2Bt_1$	42-120	5.1	0.2		41.1	32.7	26.3	22.3	14.9
$2Bt_2$	120-180	5.2	0.2		40.3	31.1	28.6	36.7	18.7

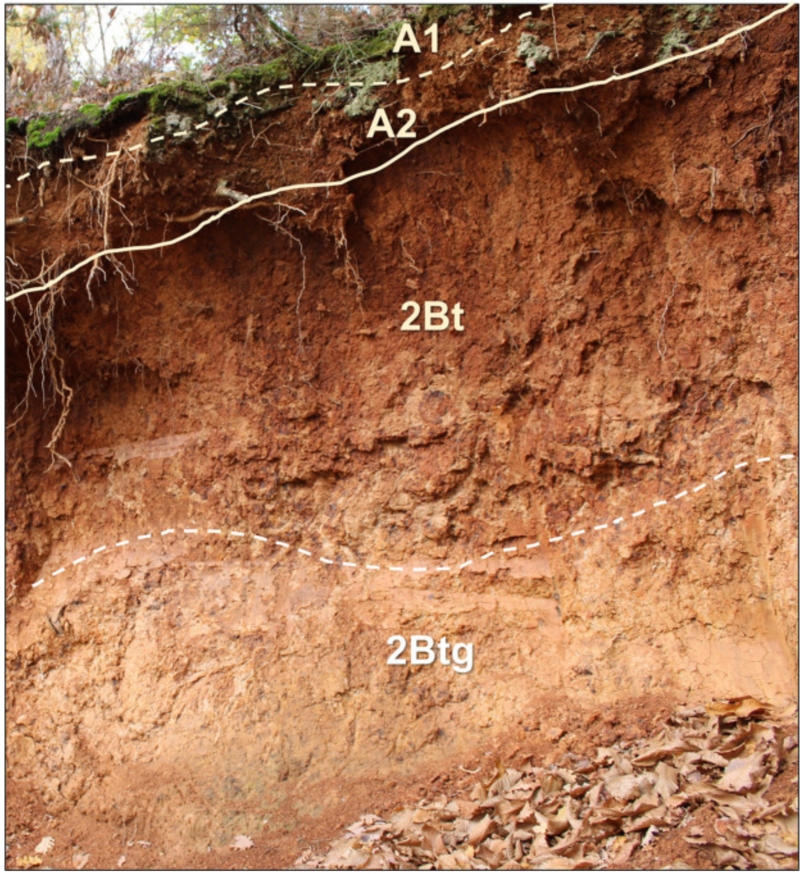

Fig. 19 - Detailed view of the soil profile.

stratigraphic homogeneity and aeolian contributions. Also, a comparable degree of weathering has been found on dated soils of more recent age, in Tuscany (Carnicelli et al., 2015).

Soil profile description and analytical data (Busoni et al., 1983; Table 5)

Altitude: 301 m asl

Slope: 2%

Land cover: due to limited chemical fertility, it highly likely that this soil has been used almost continuously as coppice wood.

Classification, WRB: Rhodic Ferric Alisol, Cutanic, Hyperdystric, Profondic (IUSS Working Group WRB, 2015)

Classification, Soil Taxonomy: Typic Paleudults, fine, mixed, mesic (Soil Survey Staff, 2003).

https://doi.org/10.3301/GFT.2023.04

Stop 3.2 - Panoramic viewpoint on the Pesciola Creek valley and look to the panorama toward SE in the Mugello Basin

Coordinates: Lat. 43°59'26.85"N, Long. 11°27'13.82"E

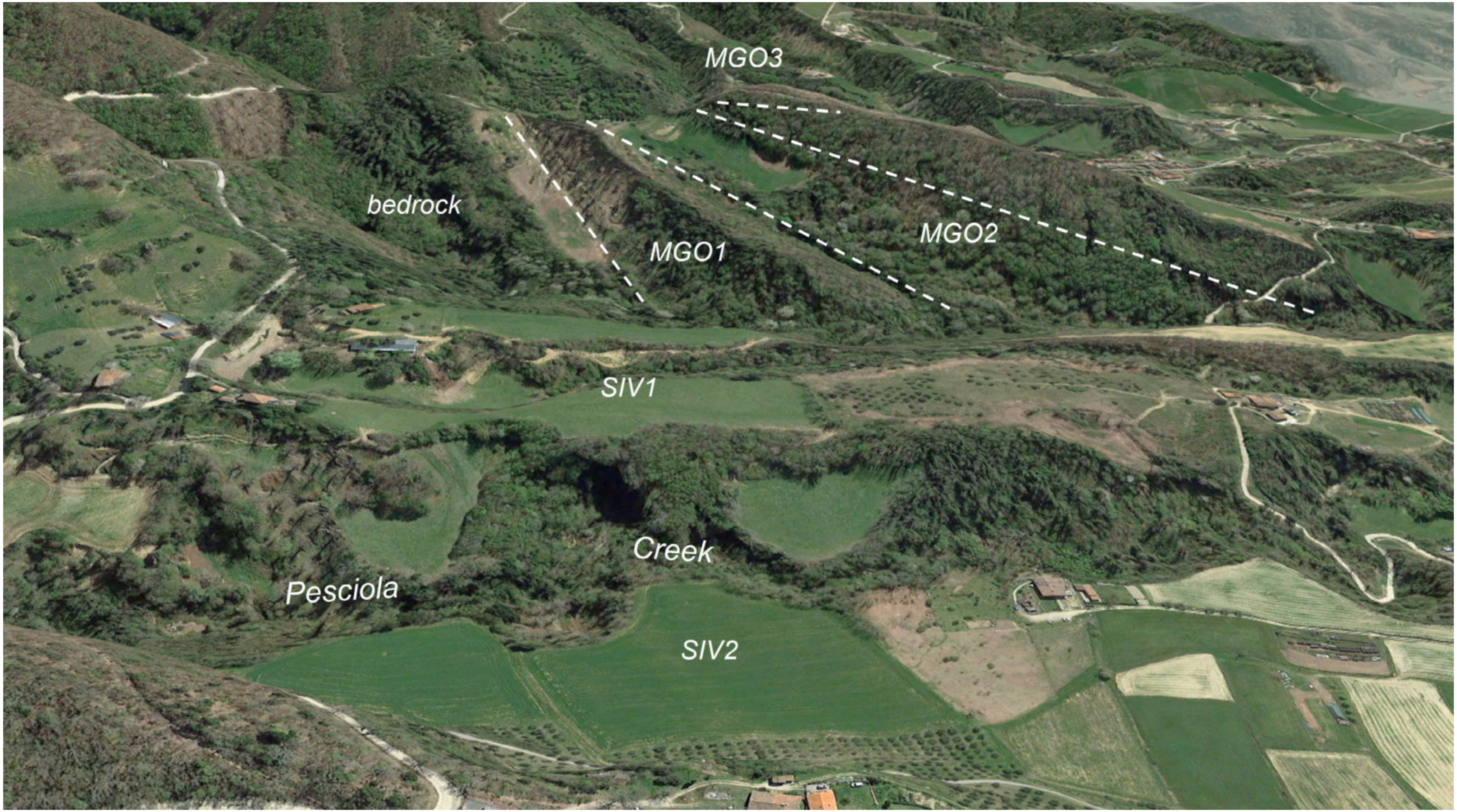

Fig. 20 - Panoramic view of the Pesciola Creek valley. Mugello Synthem (MGO): Ronta sub-synthem (MGO1); Pulicciano sub-synthem (MGO2); Farneta sub-synthem (MGO3). Sieve River Synthem (SIV): Scarperia sub-synthem (SIV1); Luco di Mugello sub-synthem (SIV2).

This panoramic viewpoint can be reached from stop 1 driving to SE and following the indications to Borgo San Lorenzo and from this town continue toward Vicchio di Mugello along the SP551. About 1.5 km turn left following the indication for Santa Maria a Vezzano. At the village, continue driving toward north for about 1 km and turn left on the dirt road that goes up the hill. Stop when you have a view on the Pesciola Creek valley and look to the panorama toward SE (Fig. 20). Differently inclined surfaces in the foreground mark the onlap of the MGO1 fan-delta conglomerate and sandstone on the steeply dipping bedrock represented by turbiditic sandstone and mudstone of the Cervarola-Falterona units. About 20° inclined surface outlines the unconformable contact between MGO1 and MGO2 fan delta deposits, the latter can be observed in the background on a vertical cliff in the Pesciola Creek valley resulting in an alternation of channelised conglomerate and muddy sandstone. A hilltop in the foreground marks the MGO3 alluvial-fan deposits capping the fluvio-lacustrine succession. The observed landscape is the geomorphic picture of a syn-tectonic succession that developed during the Early Pleistocene under the active uplift of the NE margin of the basin driven by a buried south-verging thrust fault (Fig. 16; Sani et al., 2009a). Traces of the alluvial phase are evidenced by the flat surfaces of SIV1 and SIV 2 terraces attesting to subsequent steps in the river network entrenching as the consequence of a generalised uplift of the area.

DAY 4 – THE COASTAL UPPER PLEISTOCENE SUCCESSION OF THE BARATTI GULF

Geo-morphological setting

The suggestive coastal area of Baratti, enclosed between the Populonia and the Poggio San Leonardo promontories (Fig. 21), shows a geomorphological landscape resulting from a long and complex evolution. This evolution stretches from the collisional stage in the development of the Northern Apennines orogen, dating back to the early Cenozoic, up to the recent morphological shaping of a coastal territory related to climate and sea-level variations and human frequentation. The latter was established in a stable form since the Iron Age when the Etruscans colonised the area for settling (Populonia fortified town), religious (Populonia-Baratti necropolis), and industrial (iron-copper metallurgy) purposes. The sedimentary rocks which form the substratum of the embayment belong to distinct portions of the structural stack formed by the tectonic superposition of adjacent palaeogeographic and geodynamic domains throughout the collision of the Africa and Europe continental plates. The Populonia and Poggio San Leonardo promontories are made of thick sandstones and mudstones of turbiditic origin (upper Oligocene-Lower Miocene Macigno Formation). A deformed succession of mudstone, sandstone, and limestone (Paleogene-Eocene Argille e Calcari di Canetolo Formation) is thrusted onto the Macigno Fm, representing part of the Sub-Ligurian succession. The sedimentary cover of the latter, Ligurian succession, consisting of a complex and strongly deformed succession of pelagic and turbiditic deposits including slices of lithospheric ultramafic-mafic rocks (ophiolites), is, in turn, thrusted onto the Sub-Ligurian succession. The described structural stack has been sculpted during the Neogene and the Quaternary by a complex interaction of tectonics, climate, and eustasy. The bluffs on the northern side of the embayment, made of Upper Pleistocene, rhythmically interbedded nearshore, fluvial and pedogenised slope deposits are the object of the first stop and record the more recent morphogenetic stage in the evolution of the area.

The vertical slopes, prone to mass wasting at the northern side of the Baratti embayment and further outcrops toward Poggio San Leonardo promontory (Fig. 21a), represent classic sites for the study of the coastal Quaternary of Tuscany (Cortemiglia et al., 1983; Mazzanti, 1984; Mauz, 1999; Sarti et al., 2005; Boschian et al., 2006). The most impressive feature of the succession, up to 12 metres thick, is the rhythmic alternation of yellowish hybrid calcarenites and massive reddish sandy mudstones ascribed since the early studies to glacio-eustatic fluctuations, specifically to those occurred during the Tyrrhenian (MIS 5) stage (Mazzanti, 1983; Cortemiglia at al., 1983, Fig. 22). The depositional interpretation of this cyclothemic succession referred the calcarenites ("*panchina I-III*", Cortemiglia et al., 1983, Fig. 22) to upper shoreface/beach environments marking the transgressive stages. The reddish sandy mudstones, showing soil development, were related to slope and aeolian settings established during the regressive stages (Cortemiglia et al., 1983). This depositional interpretation has been largely accepted in successive studies, though the chronological calibration has been updated by TL/OSL dating bracketing the Baratti succession between the late MIS5 and the MIS2 stages (Mauz, 1999; Fig. 22). Outcrops presented during this stop (Fig. 21b-c), will favour stratigraphic and sedimentological observation to be integrated with palaeopedological features for a reappraisal of this classic Quaternary section. Ongoing

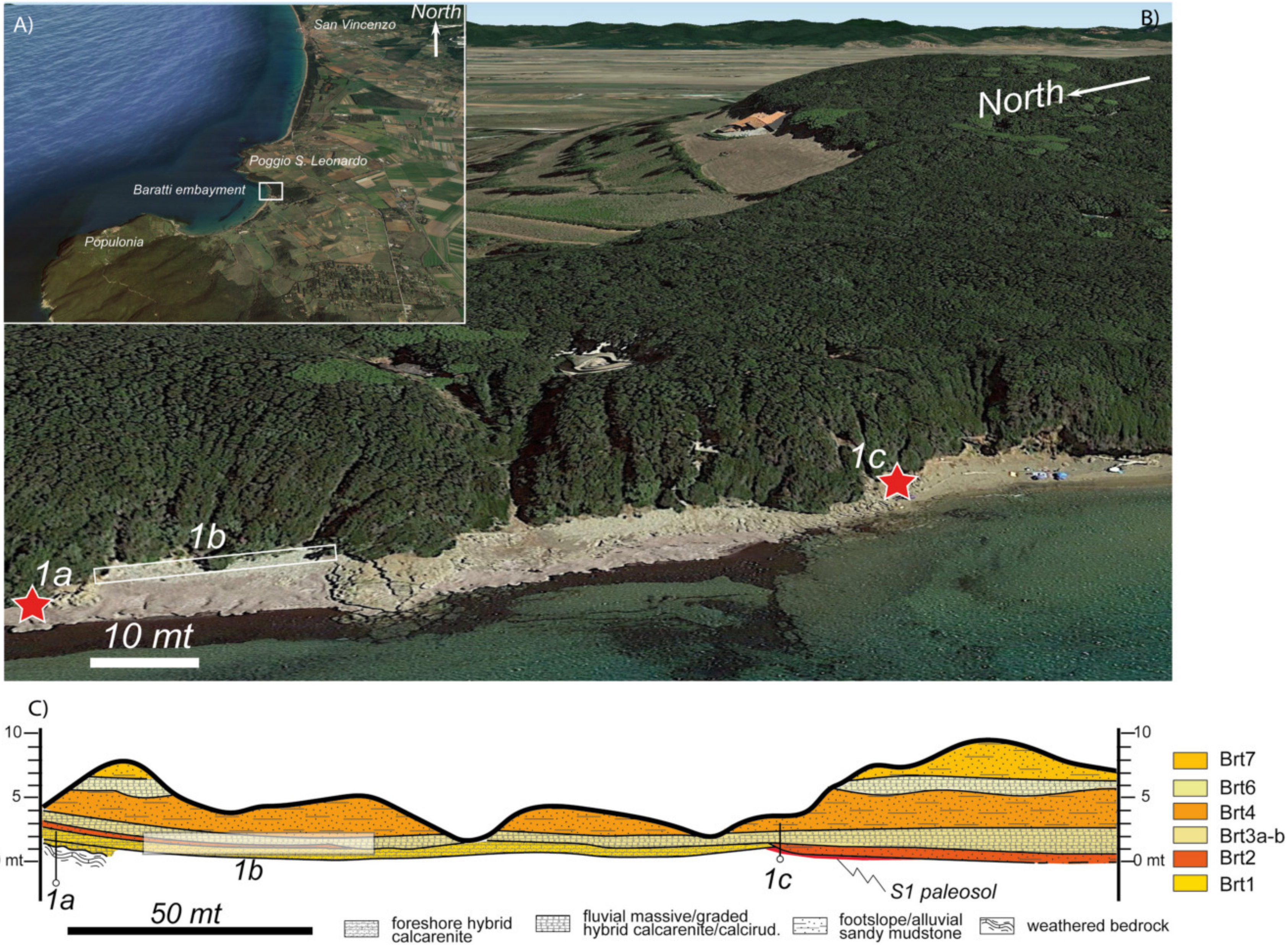

Fig. 21 - a) Oblique view of the Baratti embayment from Google Earth, the box indicates the portion of the Baratti bluffs discussed in the text; b) panoramic view looking to ENE of the sector of interest for this guide with location of the selected outcrops; c) schematic cross section along the coastal sector in b. Brt1-7 are informal stratigraphic units identified in the studied outcrops still under study.

https://doi.org/10.3301/GFT.2023.04

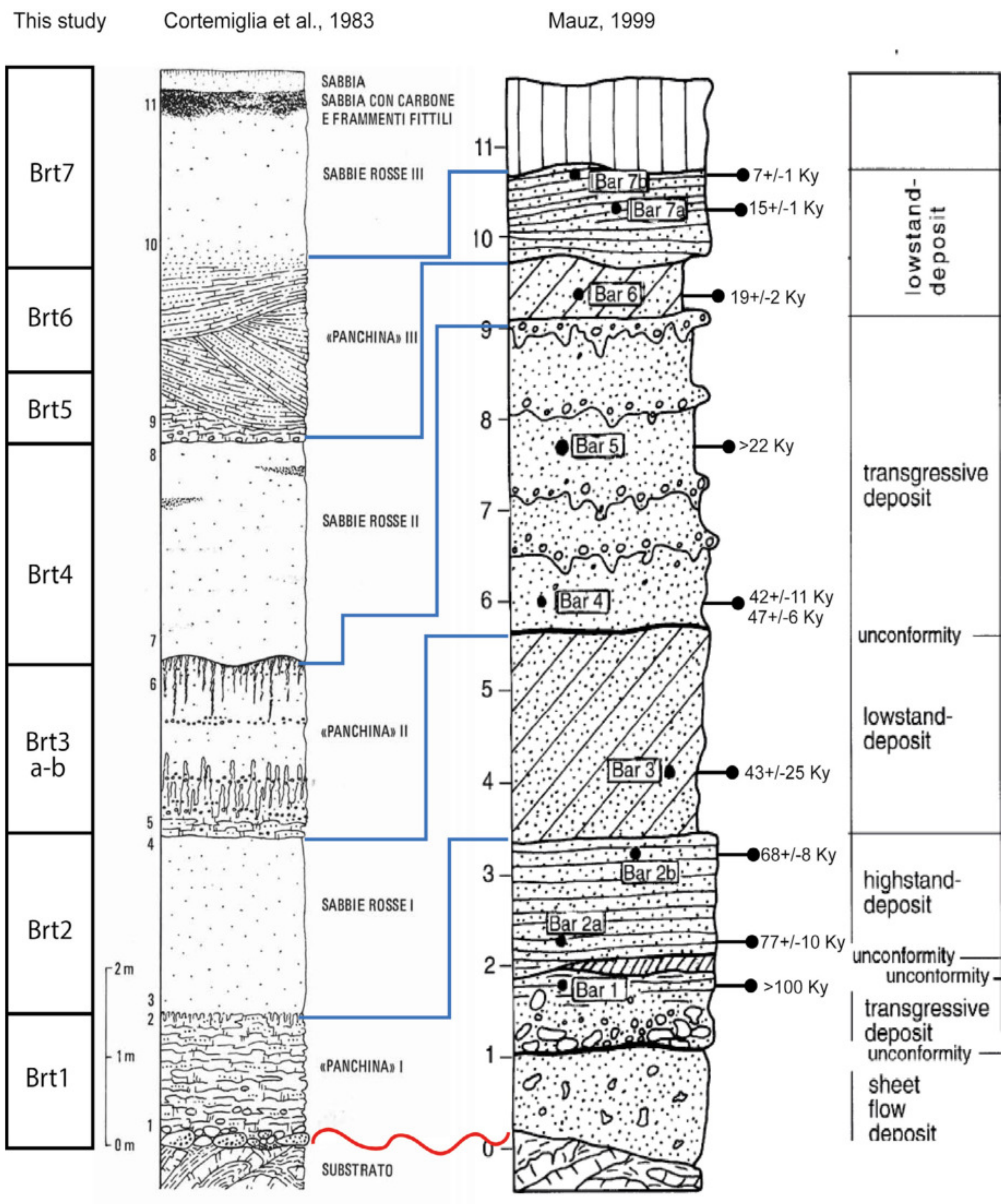

OSL analysis of samples collected in the calcarenite strata will check and eventually upgrade the chronological constraint given by Mauz (1999) up to now the only absolute calibration of this succession. The stratigraphic and facies revision resulted in a subdivision of the succession in seven main units, Brt1-7 (Fig. 21c; unit Brt5 is not discussed), which can be observed in the following exposures.

Stop 4.1 - Outcrop 1a: The basal deposits of the Baratti succession

Coordinates: Lat. 43°0'7.67"N, Long. 10°30'57.67"E

The unconformable contact of the Upper Pleistocene succession over a deeply weathered clayey bedrock (Sub-Ligurian Units) is the first striking feature visible at this outcrop (Fig. 23a-b). The basal deposits consist of two amalgamated lithologically inhomogeneous beds referred to the lower portion of unit Brt1. The lower portion of the first bed is made of polymodal cemented calcareous and arenaceous conglomerates with boulder-size extraclasts. The texture is clast supported, though with a variably content of the interstitial sandy matrix. Clasts are sub-rounded to well-rounded and, in some cases, display signs of boring organisms. Conglomerates pass abruptly upward to cemented coarse-grained through-cross laminated sandstones preserved as small pockets and hinting to the development of small 3D dunes under a tractional

Fig. 22 - Comparative stratigraphic schemes for the Upper Pleistocene succession of Baratti.

current. The second bed consists of cemented pebbly sandstones with pebble-cobble clasts floating in the sandy matrix attesting to an overall fining upward of the basal portion. The upper portion of unit Brt1 shows horizontal to low-angle laminated hybrid calcarenites sharply resting over the previous deposits.

The described bedset records a clear transgressive signal following a long period of exposure and truncation of the bedrock. The lower coarse-grained portion is referred to a small torrential creek draining the slopes and opening to the sea. Gravels were transferred by highly concentrated flood flows that during the waning stages determined the formation of small 3D dunes. The fining-up trend within this portion of the outcrop hints to decreasing stream power due to a rise in the base (sea)-level. The lithodome boring observed in some calcareous clasts attests to a transition from a supra- to an intertidal zone colonised by boring organisms, confirming the transgressive trend. The latter culminated with the establishment of a foreshore recorded by the calcarenites. From a facies point of view, the basal portion does not suggest a significant hiatus during the conglomerate deposition as reported on the base of TL/OSL chronology (Mauz, 1999; Fig. 22). Until new OSL dating, in progress, confirms or not the available chronological constraint, the described sequence refers to an almost continuous single phase of relative sea level rise.

Fig. 23 - A) Outcrop 1a: detailed view of the unconformable contact of unit Brt1 on the deeply weathered subligurian bedrock, hammer for scale; B) interpretative line-drawing of A; outcrop 1b: C) the stratigraphic relation among units Brt1, Brt2 and sub-unit Brt3a; D) particular of the Brt2 deposits with S1-S2 palaeosols, rod is 1 metre for scale; E) detail of the trough-cross laminated calcarenites of sub-unit Brt3a visible few metres southward from C, rod is 0.6 metres long; F) the deeply erosive contact of sub-unit Brt3a on unit Brt2 few metres southward E attesting to an high relief erosional contact between these deposits, rod is 1 metre long; G) outcrop 1c: panoramic view of the succession at this outcrop annotated for the stratigraphic features described in the text, person for scale.

Stop 4.2 - Outcrop 1b: The first regressive-transgressive cycle

Coordinates: Lat. 43°0’7.45”N, Long. 10°30’57.92”E

A few metres away from the previous outcrop a cut in the slope shows a rhythmic alternation of yellowish calcarenites and reddish sandy mudstones with scattered pebble strings (Fig. 23c-d). The lower calcarenite, in continuity with outcrop 1a, is overlain by reddish sandy mudstones ascribed to unit Brt2. The latter show at least two phases of soil formation (S2 and S3), evidenced by Bt horizons with common clay coatings; thin pebble layers record a colluvial setting, and concentrate around the boundary between the two pedogenised beds, which are similar except for somewhat less developed soil features and the presence of dispersed pebbles in soil S3. The upper calcarenite, sub-unit Brt3a, marks a second event ascribed to a renewed transgression which re-established a beach-shoreface setting (Cortemiglia et al., 1983). An adjacent outcrop offers details for a different depositional interpretation of the upper calcarenite. Here the calcarenites show a clear festooned bedding (Fig. 23e) represented by large trough-cross lamina sets, which attest to the development of 3D-dunes possibly in a fluvial channel network. These strata may record a more internal location along the depositional gradient established during a renewed transgression, rather than a shoreface setting as indicated in previous studies (Cortemiglia et al., 1983; Mauz, 1999). A high-relief erosive contact with unit Brt2, strongly reducing in thickness from the previous outcrop as visible a few metres away from this stop (Fig. 23f), points to the incision of a valley onto the older deposits filled by unit Brt3a. A soil Bt horizon was observed with sorted sands and clay coatings on sand grains; continuous vertical tongues of lighter colour (glossae) and rhizo-concretions are present in this horizon.

Stop 4.3 - Outcrop 1c: Lateral variations in the first regressive-transgressive cycle

Coordinates: Lat. 43° 0’3.68”N, Long. 10°30’59.79”E

This outcrop allows to observe the stratigraphic relation among units Brt1-4 (Fig. 23g). From the bottom left, a pinch-out of Brt1 calcarenites may be reconstructed despite a slope waste deposit partially covering the base of the exposure. The regressive Brt2 deposits rest abruptly over the calcarenites, whereas at the bottom right they stand over a redder sandy mudstone through an erosive contact which is ascribed to S1 palaeosol. Above, the Brt3 unit is represented by a small lens of sub-unit Brt3a calcarenites sharply overlain by sub-unit Brt3b. The latter, traceable along the main bluff of the embayment is made of graded beds of pebbly calcarenites obliterated by a characteristic network of vertical carbonate concretions hinting to pedogenic, root-driven, modification. Sub-unit Brt3b attests to the infill of a broad palaeovalley, transverse to the present coastline as indicated by the erosive contact on older deposits deepening toward SSE, seen a few metres away from this outcrop. Reddish massive sandy mudstone of unit Brt4 is visible on top of the exposure.

https://doi.org/10.3301/GFT.2023.04

Acknowledgments

The authors acknowledge the Associate Editor and two reviewers, prof. Giorgio Basilici and an anonymous reviewer for their valuable and constructive comments.

REFERENCES

Abbazzi L., Benvenuti M., Rook L., Masini F. (1995) - Biochronology of the Mugello intermontane basin (Northern Apennines, Italy). Il Quaternario, 8, 5-10.

Abbate E., Bortolotti V., Conti M., Marcucci M., Principi G., Passerini P., Treves B. (1986) - Apennines and Alps ophiolites and the evolution of western Tethys. Mem. Soc. Geol. It., 31, 23-44.

Amadori C., Toscani G., Di Giulio A., Maesano F.E., D'Ambrogi C., Ghielmi M., Fantoni R. (2019) - From cylindrical to non‐cylindrical foreland basin: Pliocene–Pleistocene evolution of the Po Plain–Northern Adriatic basin (Italy). Basin Res., 31, 991-1015.

Amorosi A. (2008) - Delineating aquifer geometry within a sequence stratigraphic framework: evidence from the Quaternary of the Po River Basin, Northern Italy. In: Amorosi A., Haq, B.U., Sabato L. (Eds.), Advances in Application of Sequence Stratigraphy in Italy. 1. GeoActa Spec. Publ., pp. 1-14.

Antonielli B. (2015) - Tectonics and mud volcanism in the Northern Apennines foothills (Italy) and in the Greater Caucasus (Azerbaijan): a satellite interferometry (InSAR) analysis. Unpublished Ph.D. Thesis, University of Pisa, 145 pp.

Arisi Rota F. and Fichera R. (1985) - Magnetic Interpretation Connected to Geo-MagneticProvinces: The Italian Case-history, Paper Presented at 47th European Association Exploration Geophysicists (EAEG) Meeting. In: Eur. Assoc. of Explor. Geophys Budapest, Hungary, 30 pp.

Bally A.W., Burbi L., Cooper C., Ghelardoni R. (1986) - Balanced sections and seismic reflection profiles across the central Apennines. Mem. Soc. Geol. It., 35, 257-310.

Barbacini G., Bernini M., Papani G., Rogledi S. (2002) - Le strutture embricate del margine appenninico emiliano fra il T. Enza e il F. Secchia - Prov. di Reggio Emilia. (con carta geologica alla scala 1:50.000). In: Regione Emilia-Romagna (Ed.), Terzo seminario sulla cartografia geologica, Bologna. Atti, pp. 64-69.

Benedetti L., Tapponnier P., Gaudemer Y., Manighetti I., Van derWoerd J. (2003) - Geomorphic evidence for an emergent active thrust along the edge of the Po Plain: the Broni-Stradella fault. J. Geophys. Res., 108(B5), 2238, https://doi.org/10.1029/2001JB001546.

Benvenuti M. (1997) - Physical stratigraphy of the fluvial-lacustrine Mugello Basin (Pleistocene, Northern Apennines, Italy). Giornale di Geologia, 59, 91-111.

Benvenuti M., Carnicelli S., Belluomini G., Dainelli N., Di Grazia S., Ferrari G.A., Iasio C., Sagri M., Ventra D., Atnafu B., Kebede S. (2002) - The Ziway–Shala lake basin (Main Ethiopian Rift, Ethiopia): a revision of basin evolution with special reference to the Late Quaternary. J. Afr. Earth Sci., 35, 247-269.

Benvenuti M. (2003) - Facies analysis and tectonic significance of lacustrine fan-deltaic successions in the Pliocene-Pleistocene Mugello Basin, Central Italy. Sediment. Geol., 157, 197-234.

Benvenuti M., Del Conte S., Scarselli N., Dominici S. (2014) - Hinterland basin development and infill through tectonic and eustatic processes: latest Messinian–Gelasian Valdelsa Basin, Northern Apennines, Italy. Basin Res., 26,387-402, http://dx.doi.org/10.1111/bre.12031

Bigi G., Bonardi G., Catalano R., Cosentino D., Lentini F., Parotto M., Sartori R., Scandone P., Turco E. (1983) - Structural Model of Italy 1:500,000, CNR Progetto Finalizzato Geodinamica.

Biju Duval B., Dercourt J., Le Pichon X. (1977) - From the Tethys Ocean to the Mediterranean Sea: plate tectonic model of the evolution of the western Alpine system. In: Biju-Duval B. and Montadert L. (Eds.), Structural History of the Mediterranean Basins. Technimp, Paris, 143-164.

Boccaletti M. and Guazzone G. (1970) - La migrazione terziaria dei bacini toscani e la rotazione dell'Appennino Settentrionale in una "zona di torsione" per deriva continentale. Mem. Soc. Geol. It., 9, 17-195.

Boccaletti M. and Guazzone G. (1972) - Gli archi appenninici, il mar Ligure ed il Tirreno nel quadro della tettonica dei bacini marginali retro-arco. Mem. Soc. Geol. It., 11(2), 201- 216.

Boccaletti M. and Guazzone G. (1974) - Remnant arcs and marginal basins in the Cainozoic development of the Mediterranean. Nature, 252, 18-21.

Boccaletti M., Elter P., Guazzone G. (1971) - Plate tectonic models for the development of the Western Alps and Northern Apennines. Nat., Phys. Scr., 234, 108-111.

Boccaletti M., Coli M., Decandia F.A., Giannini E., Lazzarotto A. (1980) - Evoluzione dell"Appennino settentrionale secondo un nuovo modello strutturale. Mem. Soc. Geol. It., 21, 359-373.

https://doi.org/10.3301/GFT.2023.04

Boccaletti M., Bonini M., Moratti G., Sani F. (1999) - Compressive Neogene –Quaternary tectonics in the hinterland area of the Northern Apennines. In: Boccaletti, M., Dahmani, M. (Eds.), Neogene Sedimentation and Tectonics in the Western Mediterranean. J. Pet. Geol., 22, 3760.

Boccaletti M., Bonini M., Corti G., Gasperini P., Martelli L., Piccardi L., Tanini C., Vannucci G. (2004) - In: Regione Emilia-Romagna-CNR (Ed.), Seismotectonic Map of the Emilia-Romagna Region, 1:250,000. SELCA, Firenze, Italy.

Boccaletti M., Corti G., Martelli L. (2011) - Recent and active tectonics of the external zone of the Northern Apennines (Italy). Int. J. Earth Sci., 100, 1331-1348. https://link.springer.com/article/10.1007/s00531-010-0545-y.

Bonini M. (2013) - Fluid seepage variability across the external Northern Apennines (Italy): structural controls with seismotectonic and geodynamic implications. Tectonophysics, 590, 151-174.

Bonini M. and Sani F. (2002) - Extension and compression in the Northern Apennines (Italy) hinterland: Evidence from the Late Miocene-Pliocene Siena-Radicofani Basin and relations with basement structures. Tectonics, 21(3), 1010, https://doi.org/10.1029/2001TC900024.

Bonini M., Moratti G., Sani F. (1999) - Evolution and depocenter migration in thrust-top basins: inferences from the Messinian Velona Basin (Northern Apennines, Italy). Tectonophysics, 304, 95-108.

Bonini M., Moratti G., Sani F., Balestrieri M.L. (2013) - Compression-to-extension record in the Plio-Pleistocene Upper Valdarno Basin (Northern Apennines, Italy): structural and thermochronological constraints. Ital. J. Geosci., 132, 54-80, https://doi.org/10.3301/IJG.2011.18.

Bonini M., Sani F., Stucchi E., Moratti G., Benvenuti M., Menanno G., Tanini C. (2014) - Late Miocene shortening of the Northern Apennines back–arc. J. Geodynamics, 74, 1-31, http://dx.doi.org/10.1016/j.jog.2013.11.002

Bortolotti V. and Principi G. (2005) - Tethyan ophiolites and Pangea break-up. Isl. Arc, 14, 442-470, https://doi.org/10.1111/j.1440-1738.2005.00478.x.

Bortolotti V., Fazzuoli M., Pandeli E., Principi G., Babbini A., Corti S. (2001) - Geology of central and eastern Elba island, Italy. Ofioliti 26 (2a), 97-150.

Bortolotti V., Poccianti C., Principi G., Sani F. (2015) - Note illustrative della Carta Geologica d'Italia alla scala 1:50.000. Foglio 264 - Borgo San Lorenzo. ISPRA - Servizio Geologico d'Italia, 103 pp.

Boschian G., Bossio A., Dall'Antonia B., Mazzanti R. (2006) - Il Quaternario della Toscana costiera. Studi costieri, 12, 207 pp.

Burrus J. (1984) - Contribution to a geodynamic synthesis of the Provençal basin (north-western Mediterranean). Mar. Geol., 55, 247-269

Busoni E., Dimase A.C.; Sanesi G. (1983) - Risultati sperimentali per la valutazione dei suoli agricoli e forestali in Toscana. Consiglio Nazionale delle Ricerche. Centro di Studio per la Genesi e la Cartografia e Classificazione del Suolo.

Capacci C. (1920) - Osservazioni geotettoniche sul terremoto mugellano del 29 Giugno 1919. Atti della R. Acc. dei Georg., Firenze, 182-194.

Carminati E. and Doglioni C. (2012) - Alps *vs.* Apennines: the paradigm of a tectonically asymmetric Earth. Earth-Sci. Rev., 112, 67-96.

Carnicelli S. and Costantini E.D. (2013) - Time as a soil forming factor and age of Italian soils. In: Costantini, E.D., Dazzi, C. (Eds.), The Soils of Italy. Springer, pp. 93-104.

Carnicelli S., Mirabella A., Cecchini G., Sanesi G. (1997) - Weathering of Chlorite to a Low-Charge Expandable Mineral in a Spodosol on the Apennine Mountains, Italy. Clay Clay Miner., 45, 28-41.

Carnicelli S., Benvenuti M., Andreucci S., Ciampalini R. (2015) - Late Pleistocene relic Ultisols and Alfisols in an alluvial fan complex in coastal Tuscany. Quat. Int., 376, 163-172.

Carnicelli S., Caporale L., Marchi N., Iasio C., Ferrari G.A., Guermandi M., Tarocco P. (2003) - Paleosols of the Apenninic margin, a case study in the Reggio-Emilia Province. In: Regione Emilia Romagna (Ed.), Note For Field Excursion. Regione Emilia Romagna, Servizio Geologico Sismico e dei Suoli, Bologna, Italy.

Cassano E., Anelli L., Cappelli V., La Torre P. (1998) - Interpretation of Northern-Apennine magnetic and gravity data in relation to the profile Crop-03. Mem. Soc. Geol. It., 52, 413-425.

Cassinis R., Scarascia S., Lozej A. (2005) - Review of seismic wide-angle reflection-refraction (WARR) results in the Italian Region (1956–1987). Chapter 2 –Lithospheric tectono-stratigraphic setting of the Ligurian Sea – Northern Apen-nines – Adriatic Foreland from Integrated CROP Seismic Data. In: Finetti I. (Ed.), CROP Project – Deep seismic exploration of the Central Mediterranean and Italy,Atlases in Geoscience 1. Elsevier B.V., ISBN 0-444-50693-4, pp. 31-55.

Castiglioni G.B. and Pellegrini G.B. (2001) - Note illustrative della carta geomorfologica della Pianura Padana: Illustrative Notes of the Geomorphological Map of Po Plain (Italy). Edited by G.B. Castiglioni, G.B. Pellegrini. Comitato glaciologico italiano.

Castiglioni G.B., Ajassa R., Baroni C., Biancotti A., Bondesan A., Bondesan M., Brancucci G., Castaldini D., Castellaccio E., Cavallin A., Cortemiglia F., Cortemiglia G.C., Cremaschi M., Da Rold O., Elmi C., Favero V., Ferri R., Gandini F., Gasperi G., Giorgi G., Marchetti G., Marchetti M., Marocco R., Meneghel M., Motta M., Nesci O., Orombelli G., Paronuzzi P., Pellegrini G.B., Pellegrini L., Rigoni A., Sommaruga M., Sorbini L., Tellini C., Turrini M.C., Vaia F., Vercesi P.L., Zecchi R., Zorzin R. (1997) - Carta Geomorfologica della Pianura Padana. 3 Fogli alla scala 1:250.000.

Cerrina Feroni A., Ottria G., Martinelli P., Martelli L. (2002) - Carta Geologico-Strutturale dell'Appennino Emiliano-Romagnolo. S.E.L.C.A, Firenze.

Chiarabba C., Jovane L., Di Stefano R. (2005) - A new view of Italian seismicity using 20 years of instrumental recordings. Tectonophysics 395, 251-268.

Cortemiglia G.C., Mazzanti R., Parea G.C. (1983) - Geomorfologia della Baia di Baratti (Livorno-Toscana) e della sua spiaggia. Geogr. Fis. Dinam. Quat., 6: 148-173.

Cremaschi M. (1987) - Paleosols and Vetusols in the Central Po Plain (northern Italy): A Study in Quaternary Geology and Soil Development. Unicopli, Milano, Italy, pp. 306.

Cremaschi M., Zerboni A., Nicosia C., Negrino F., Rodnight H., Spötl C. (2015) - Age, soil-forming processes, and archaeology of the loess deposits at the Apennine margin of the Po plain (northern Italy): new insights from the Ghiardo area. Quat. Int., 376, 173-188.

Della Vedova B., Bellani S., Pellis G., Squarci P. (2001) - Deep temperatures and surface heat flow distribution. In: Vai, G.B., Martini, I.P. (Eds.), Anatomy of an Orogen: The Apennines and the Adjacent Mediterranean Basins. Kluwer AcademicPublisher, pp. 65-76.

Dewey J.F., Pitman W.C., Ryan W.B.F., Bonnin J. (1973) - Plate Tectonics and the evolution of Alpine system. Geol. Soc. Am. Bull., 84, 3137-3180.

DISS Working Group (2021) - Database of Individual Seismogenic Sources (DISS), Version 3.3.0: A Compilation of Potential Sources for Earthquakes Larger Than M 5.5 in Italy and Surrounding Areas, INGV (Istituto Nazionale di Geofisica e Vulcanologia).

Doglioni C. (1991) - A proposal for the kinematic modelling of W-dipping subduction: possible applications to the Tyrrhenian-Apennines system. Terra Nova 3, 423-434.

Faccenna C., Funiciello F., Giardini D., Lucente P. (2001) - Episodic back-arc extension during restricted mantle convection in the Central Mediterranean. Earth Planet. Sci. Lett., 187, 105-116. https://doi.org/10.1016/S0012-821X(01)00280-1.

Fidolini F. and Andreetta A. (2013) - Integrating sedimentological and palaeopedological data for palaeoenvironmental reconstruction: Examples from the Plio-Pleistocene Upper Valdarno Basin (Northern Apennines, Italy). Ital. J. Geosci., 132(1), 149-166

Finetti I. and Del Ben A. (1986) - Geophysical study of the Tyrrhenian opening. Boll. Geof. Teor. Appl. 28 (110), 75-156.

Finetti I.R., Boccaletti M., Bonini M., Del Ben A., Geletti R., Pipan M., Sani F. (2001) - Crustal section based on CROP seismic data across the North Tyrrhenian-Northern Apennines-Adriatic Sea. Tectonophysics, 343, 135-163.

GeMiNa (1962) - Ligniti e torbe dell'Italia continentale. Roma, pp. 61-75.

Gunderson K.L., Pazzaglia F.J., Picotti V., Anastasio D.A., Kodama K.P., Rittenou R.T., Frankel K.F., Ponza A., Berti C., Negri A., Sabbatini A. (2014) - Unravelling tectonic and climatic controls on synorogenic growth strata (Northern Apennines, Italy). Geol. Soc. Am. Bull., 126-3(4), 532-552.

IUSS Working Group WRB (2015) - World Reference Base for Soil Resources 2014, Update 2015. International Soil Classification System for Naming Soils and Creating Legends for Soil Maps. World Soil Resources Reports No. 106, Rome: FAO.

Livani M., Scrocca D., Arecco P., Doglioni C. (2018) - Structural and stratigraphic control on salient and recess development along a thrust belt front: The Northern Apennines (Po Plain, Italy). Solid Earth, 123, 4360-4387, https://doi.org/10.1002/2017JB015235.

Maestrelli D., Benvenuti M., Bonini M., Carnicelli S., Piccardi L., Sani F. (2018) - The structural hinge of a chain-foreland basin: Quaternary activity of the Pede-Apennine Thrust front (Northern Italy). Tectonophysics, 723, 117-135.

Malinverno A. and Ryan W.B.F. (1986) - Extension in Tyrrhenian Sea and shortening in the Apennines as result of arc migration driven by sinking of the lithosphere. Tectonics, 5, 227-254.

Marroni M., Meneghini F., Pandolfi L. (2017) - A revised subduction inception model to explain the Late Cretaceous, double-vergent orogen in the precollisional western Tethys: Evidence from the Northern Apennines. Tectonics, 36, https://doi.org/10.1002/2017TC004627.

Martelli L., Bonini M., Calabrese L., Corti G., Ercolessi G., Molinari F.C., Piccardi L., Pondrelli S., Sani F., Severi P. (2017a) - Note Illustrative della Carta sismotettonica della Regione Emilia-Romagna ed aree limitrofe., 93 pp. ISBN 978-88-8186-013-5.

Martelli L., Santulin M., Sani F., Tamaro A., Bonini M., Rebez A., Corti G. and Slejko D. (2017b) - Seismic hazard of the Northern Apennines based on 3D seismic sources. J. Seismol., 21(5), 1251-1275, https://doi.org/10.1007/s10950-017-9665-1.

Martini I.P. and Sagri M. (1993) - Tectono-sedimentary characteristics of Late Miocene-Quaternary extensional basins of the Northern Apennines, Italy. Earth Sci. Rev., 34, 197-233.

Martini M., Sibilia E., Croci S., Cremaschi M. (2001) - Thermoluminescence (TL) dating of burnt flints: problems, perspectives and some examples of application. J. Cult. Herit., 2, 179-190.

Mauz B. (1999) - Late Pleistocene records of littoral processes at the Tyrrenian Coast (Central Italy): depositional environments and luminescence chronology. Quat. Sci. Rev., 18, 1173-1184.

Mazzanti R. (1984) - Il punto sul Quaternario della fascia costiera e dell"Arcipelago di Toscana. Boll. Soc. Geol. It., 102,419-556.

Molli G., Carlini M., Vescovi P., Artoni A., Balsamo F., Camurri F., Clemenzi L., Storti F., Torelli L. (2018) - Neogene 3-D structural architecture of the north-west Apennines: The role of the low-angle normal faults and basement thrusts. Tectonics, 37, https://doi.org/10.1029/2018TC005057.

Mongelli F., Pialli G., Zito G. (1998) - Tectonic subsidence, heat flow and uplift inTuscany: a new geodynamic and geothermal approach. Mem. Soc. Geol. It., 52, 275-282.

Montone P., Mariucci M.T., Pierdominici S. (2012) - The Italian present day stress map, Geophys. J. Int., 189(2), 705-716.

Moratti G. and Bonini M. (1998) - Structural development of the Neogene Radicondoli-Volterra and adjoining hinterland basins in Western Tuscany (NorthernApennines, Italy). Geol. J., 33, 223-241.

NACSM - North American Commission on Stratigraphic Nomenclature (2005) - North American Stratigraphic Code. AAPG Bull., 89(11), 1547-1591.

Pavesi M. (2008) - Architettura stratigrafica dei depositi medio e tardo quaternari del bacino padano, finalizzata alla caratterizzazione geometrica degli acquiferi. Unpublished Ph.D. Thesis, University of Bologna, pp. 217.

Pellegrini M. and Vezzani L. (1978) - Faglie attive in superficie nella Pianura Padana presso Correggio (Reggio Emilia) e Massa Finalese (Modena). Geogr. Fis. Dinam. Quat., 1, 141-149

Pieri M. and Groppi G. (1981) - Subsurface geological structure of the Po Plain, Italy, in *Un* Progetto Finalizzato Geodinamica, p. 414, C.N.R. Publications.

Pizziolo M., Segadelli S., Vaiani S.C. Maffei M., Vigliotti L., Di Cocco I., Bassetti M.A. (2016) - Note Illustrative della Carta Geologica d'Italia alla scala 1:50.000, Foglio 200, Reggio nell'Emilia. Servizio geologico d'Italia, pp. 110.

Pondrelli S., Salimbeni S., Ekstrom G., Morelli A., Gasperini P., Vannucci G. (2006) - The Italian CMT dataset from 1977 to the present. Phys. Earth Planet. In., 159(3-4), 286-303.

Ponziani F., De Franco R., Minelli G., Biella G., Federico C., Pialli G. (1995) - Crustal shortening and duplication of the Moho in the Northern Apennines: a view from the seismic refraction data. Tectonophysics, 252, 391-418.

RER (Regione Emilia-Romagna), ENI-AGIP (1998) - In: Dio, Di (Ed.), Riserve idriche sotterranee della regione Emilia-Romagna. S.EL.CA., Firenze, pp. 120.

Riba O. (1976) - Syntectonic unconformities of the Alto Caderner, Spanish Pyrenees: a genetic interpretation. Sediment. Geol., 15, 213-233.

Sagri M., Bartolini C., Billi P., Ferrari G., Benvenuti M., Carnicelli S., Barbano F. (2008) - Latest Pleistocene and Holocene river network evolution in the Ethiopian lakes region. Geomorphology, 94, 1-2.

Sanesi G. (1965) - Geologia e morfologia dell'antico bacino lacustre del Mugello – Firenze. Boll. Soc. Geol. It., 84(3), 169-252.

Sani F., Bonini M., Piccardi L., Vannucci G., Delle Donne D., Benvenuti M., Moratti G., Corti G., Montanari D., Sedda L. Tanini C. (2009a) - Late Pliocene-Quaternary evolution of outermost hinterland basins of the Northern Apennines (Italy), and their relevance to active tectonics. Tectonophysics, 476, 336-356.

Sani F., Bonini M., Cerrina Feroni A., Mazzarini F., Moratti G., Musumeci G., Corti G., Iatta F., Ellero A. (2009b) - Messinian-Early Pliocene crustal shortening along the Tyrrhenian margin of Tuscany, Italy. Ital. J. Geosci., 128, 2, 593-604.

Sani F., Bonini M., Moratti G., Corti G., Montanari D., Del Ventisette C. (2016) - The structural evolution of the Radicondoli–Volterra Basin and the relationships with magmatism of southern Tuscany (Italy). Geothermics, 59, 38-55, https://doi.org/10.1016/j.geothermics.2015.10.008.

Sarti G., Zanchetta G., Ciulli L., Colonese A. (2005) - Late Quaternary oligotypical non-marine mollusc fauna from southern Tuscany: climatic and stratigraphyc implications. GeoActa, 4, 159-167.

Scarascia S., Cassinis R., Federici F. (1998) - Gravity modeling of deep structures inthe northern-central Apennines. Mem. Soc. Geol. It., 52, 231-246.

Schaetzl R.J., Thompson M.L. (2015) - Soil: Genesis and Geomorphology, 2nd ed. Cambridge University Press, Cambridge, UK, pp. 827.

Scholle P.A. (1970) - The Sestri–Voltaggio Line: a transform fault induced tectonic boundary between the Alps and the Apennines. Am. J. Sci., 269, 343-359.

Scrocca D., Carminati E., Doglioni C., Marcantoni D. (2007) - Slab retreat and active shortening along the Central-Northern Apennines, in Thrust Belts and Foreland Basins: Frontiers in Earth Sciences, Springer, pp. 471-487.

Schoeneberger P.J., Wysocki D.A., Benham E.C., Soil Survey Staff (2012) - Field Book for Describing and Sampling Soils, Version 3.0. Natural Resources Conservation Service, National Soil Survey Center, Lincoln. https://www.nrcs.usda.gov/sites/default/files/2022-09/field-book.pdf.

Serpelloni E., Anzidei M., Baldi P., Casula G., Galvani A. (2005) - Crustal velocity and strain-rate fields in Italy and surrounding regions: new results from the analysis of permanent and non-permanent GPS networks. Geophys. J. Int., 161, 861-880, http://dx.doi.org/10.1111/j.1365-246X.2005.02618.x.

Serpelloni E., Vannucci G., Pondrelli S., Argnani A., Casula G., Anzidei M., Baldi P., Gasperini P. (2007) - Kinematics of the Western Africa-Eurasia plate boundary from focal mechanisms and GPS data. Geophys. J. Int. 169, 1180-1200, http://dx.doi.org/10.1111/j.1365-246X.2007.03367.x.

Serri G., Innocenti F., Manetti P. (1993) - Geochemical and petrological evidence ofthe subduction of delaminated Adriatic continental lithosphere in the genesis of the Neogene-Quaternary magmatism of central Italy. Tectonophysics, 223,117-147.

Soil Survey Staff (1999) - Soil taxonomy: A basic system of soil classification for making and interpreting soil surveys. 2nd edition. Natural Resources Conservation Service. U.S. Department of Agriculture Handbook 436.

Soil Survey Staff (2003) - Keys to Soil Taxonomy (9th ed.), United States Department of Agriculture, Washington.

USDA-NRCS (2012) - National Soil Survey Handbook. No. 430, US Department of Agriculture, USDA, Washington DC, https://www.nrcs.usda.gov/resources/guides-and-instructions/national-soil-survey-handbook.

Vai G.B. (2001) - Structure and stratigraphy: an overview. In: G.B. Vai, I.P.Martini (Eds.), Anatomy of an orogen: Northern Apennines and Adjacent Mediterranean Basins. Kluwer Academic Publ., Dordrecht, 15-32

Vannoli, P., Burrato, P., Valensise, G. (2015) - The Seismotectonics of the Po Plain (Northern Italy): tectonic diversity in a blind faulting domain. Pure Appl. Geophys. 72-5, 1105–1142, http://dx.doi.org/10.1007/s00024-014-0873-0.

Zapata T.R. and Allmendinger R.W. (1996) - Growth stratal records of instantaneous and progressive limb rotation in the Pre-cordilleran thrust belt and Bermejo basin. Tectonics 15, 1065-1083.

Zuffetti C. and Bersezio R. (2020) - Morphostructural evidence of Late Quaternary tectonics at the Po Plain- Northern Apennines border (Lombardy, Italy). Geomorphology, 364, 107245

Zuffetti C., Trombino L., Zembo I., Bersezio R. (2018) - Soil evolution and origin of landscape in a late Quaternary tectonically mobile setting: The Po Plain-Northern Apennines border in Lombardy (Italy). Catena, 171, 376-397.

Manuscript received 15 January 2023; accepted 13 May 2023; published online 27 June 2023;
editorial responsibility and handling by S. Fabbi